

MICROCOPY RESOLUTION TEST CHART
NATIONAL BUREAU OF STANDARDS-1963-A

ATOMIC TRANSPORT
IN METALLIC GLASSES

by

R.C. Cammarata,
A.L. Greer,
F. Spaepen and
S.S. Tsao

(17)

Office of Naval Research
Contract N00014-77-C-0002 NR-039-136

ATOMIC TRANSPORT
IN METALLIC GLASSES

by

R.C. Cammarata,
A.L. Greer,
F. Spaepen and
S.S. Tsao

40407

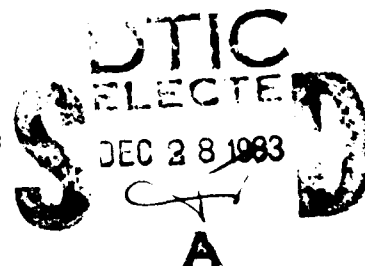
Technical Report No. 24

This document has been approved for public release and sale; its distribution is unlimited. Reproduction in whole or in part is permitted by the U. S. Government.

November 1983

The research reported in this document was made possible through support extended the Division of Applied Sciences, Harvard University, by the Office of Naval Research under Contract Number N00014-77-C-0002.

Division of Applied Sciences
Harvard University · Cambridge, Massachusetts



REPORT DOCUMENTATION PAGE

READ INSTRUCTIONS BEFORE COMPLETING FORM

1. REPORT NUMBER Technical Report No. 24		2. GOVT ACCESSION NO. AD-A136363		3. RECIPIENT'S CATALOG NUMBER	
4. TITLE (and Subtitle) ATOMIC TRANSPORT IN METALLIC GLASSES		5. TYPE OF REPORT & PERIOD COVERED Interim Report			
7. AUTHOR(s) R.C. Cammarata, A.L. Greer, F. Spaepen, S.S. Tsao		6. PERFORMING ORG. REPORT NUMBER			
9. PERFORMING ORGANIZATION NAME AND ADDRESS Division of Applied Sciences Harvard University Cambridge, MA 02138		8. CONTRACT OR GRANT NUMBER(s) N00014-77-C-0002			
11. CONTROLLING OFFICE NAME AND ADDRESS		10. PROGRAM ELEMENT, PROJECT, TASK AREA & WORK UNIT NUMBERS			
		12. REPORT DATE November 1983			
		13. NUMBER OF PAGES			
14. MONITORING AGENCY NAME & ADDRESS (if different from Controlling Office)		15. SECURITY CLASS. (of this report) Unclassified			
		15a. DECLASSIFICATION/DOWNGRADING SCHEDULE			
16. DISTRIBUTION STATEMENT (of this Report) This document has been approved for public release and sale; its distribution is unlimited. Reproduction in whole or in part is permitted by the U.S. Government.					
17. DISTRIBUTION STATEMENT (of the abstract entered in Block 20, if different from Report)					
18. SUPPLEMENTARY NOTES					
19. KEY WORDS (Continue on reverse side if necessary and identify by block number) atomic diffusion, viscosity, creep, amorphous metals, compositionally modulated films, structural relaxation, iso-configurational flow, bimolecular kinetics, Stokes-Einstein relation					
20. ABSTRACT (Continue on reverse side if necessary and identify by block number) The viscosity of glassy Pd _{77.5} Cu ₆ Si _{16.5} near T _g has bimolecular relaxation kinetics. A new determination of the equilibrium is reported, which is an order of magnitude higher than literature values. The iso-configurational temperature dependence is found to depend on thermal history. Diffusion measurements in compositionally modulated films have been made. Reported here are: iso-configurational diffusivities, relaxation kinetics, and modulation wavelength dependence. The existence of a gradient energy coefficient in metallic glasses has been established. The diffusivity is about two orders of magnitude higher					

PREFACE

This report combines four papers on atomic transport in amorphous metals, which have recently been published or are currently in press.

They are:

1. S.S. Tsao and F. Spaepen, "Models for Iso-Configurational Flow and Viscosity Relaxation in Metallic Glasses," Amorphous Materials, Modeling of Structure and Properties (ed. V. Vitek), New York: TMS-AIME (1983), p. 323.
2. A.L. Greer, "Compositionally Modulated Metallic Glasses," Modulated Structure Materials (ed. T. Tsakalakos), NATO ASI Series, Applied Science, The Hague: Nijhoff, in press.
3. R.C. Cammarata and A.L. Greer, "Interdiffusion Studies in Metallic Glasses Using Compositionally Modulated Thin Films," Proceedings of the Fifth International Conference on Liquid and Amorphous Metals, Los Angeles, California, August 15-19, 1983. To be published in J. Non-Cryst. Solids.
4. A.L. Greer, "Atomic Transport and Structural Relaxation in Metallic Glasses," Proceedings of the Fifth International Conference on Liquid and Amorphous Metals, Los Angeles, California, August 15-19, 1983. To be published in J. Non-Cryst. Solids.

Accession No.	
NTIS USMI	<input checked="" type="checkbox"/>
DTIC TAB	<input type="checkbox"/>
Unannounced	<input type="checkbox"/>
Justification	
By	
Distribution	
Availability	
Dist	

AT



MODELS FOR ISO-CONFIGURATIONAL FLOW AND VISCOSITY RELAXATION

IN METALLIC GLASSES

Sylvia S. Tsao and Frans Spaepen

Division of Applied Sciences
Harvard University
Cambridge, Massachusetts 02138
U.S.A.

The non-linear viscosity increase as a result of structural relaxation near equilibrium has been measured for amorphous $Pd_{77.5}Cu_8Si_{16.5}$. The data were analyzed by comparing them with the predictions of unimolecular and bimolecular relaxation models, with the bimolecular model giving the better fit. These fits also gave new values of the equilibrium viscosity, which are about one order of magnitude higher than earlier determinations that did not take relaxation fully into account. The viscosity change as a result of crystallization was found to be satisfactorily described by Einstein's equation for the effective viscosity of a medium containing a small volume fraction of rigid particles.

The isocconfigurational temperature dependence of the viscosity of two specimens pre-annealed under different conditions has been shown to be different. Comparison of the results, together with earlier determination shows that the annealing history of the glass must be taken into account in the modeling of the effect of iso-configurational temperature changes on the viscosity.

Introduction

Structural imperfections or "defects" in amorphous materials are local deviations from its ideal structure, which is defined - conceptually only, since it is experimentally inaccessible - as the configuration of the amorphous system in internal equilibrium at absolute zero temperature. As in crystalline materials, atomic transport processes, such as diffusion and plastic flow, are thought to be governed by the nature, concentration and rearrangement frequency of these defects. The lack of translational order in amorphous materials, however, makes modeling of their defects as direct analogues of those in crystals inappropriate. Most atomic scale defect modeling therefore involves analyzing or perturbing amorphous cluster models, using static relaxation or molecular dynamics. The ultimate test of any defect model, however, is its usefulness in characterizing atomic transport, and its ability to account for the equilibrium and non-equilibrium variations in the atomic transport coefficients and the kinetics of structural relaxation. Phenomenological models, such as the bimolecular kinetic law for the time dependence of structural relaxation or the Fulcher-Vogel law for the temperature dependence of the equilibrium viscosity, are useful for bringing out some of the essential features of the atomic transport process against which microscopic models must be tested. In this paper, recent developments in our experimental and phenomenological modeling work on the viscosity of metallic glasses are described.

The atomic transport coefficients, such as the diffusivity, D , and the shear viscosity, η , depend very sensitively on the structural state of the glass. For example, Taub and Spaepen (1) have measured increases in η of several orders of magnitude as a result of structural relaxation during annealing of $\text{Pd}_{82}\text{Si}_{18}$. In the temperature range they studied (424-537K), the isothermal rate of viscosity increase, $\dot{\eta}$, was observed to be constant in time. This behavior could be modeled as a bimolecular annihilation process of flow defects, of concentration n_f , at special relaxation sites, of concentration n_s proportional to n_f (2). At higher temperatures (near the glass transition temperature, T_g), however, η is expected to decrease with time and eventually become zero when the viscosity, $\eta_{\text{eq}}(T)$, characteristic of the metastable equilibrium configuration at that temperature is reached. That a unique $\eta_{\text{eq}}(T)$ exists for a metallic glass has been demonstrated by the work of Chen and Turnbull on $\text{Au}_{0.77}\text{Ge}_{0.136}\text{Si}_{0.094}$ (3). In most metallic glasses, it is impossible to determine the equilibrium viscosity experimentally, due to the onset of rapid crystallization long before the sample has reached its metastable equilibrium configuration. In this paper we report results of experiments near equilibrium on as-quenched $\text{Pd}_{77.5}\text{Cu}_6\text{Si}_{16.5}$ samples, in which the crystallization kinetics around T_g are relatively slow. A decreasing $\dot{\eta}(t)$ was observed, and used as a test for two phenomenological relaxation models.

The temperature dependence of the non-equilibrium viscosity is studied in so-called "isoconfigurational" experiments. Although the viscosity of the glass increases continually and irreversibly due to structural relaxation, and even linearly with time at low temperatures, the relative rate of increase of viscosity, $d(\ln\eta)/dt$ continually decreases. This makes it possible, for sufficiently annealed samples, to make measurements at different temperatures over a time period during which a negligible amount of further relaxation occurs, so that the viscosity is reproducible upon cycling of the temperature. In a previous paper (4) we reported results of isoconfigurational measurements on a PdCuSi sample, which were in apparent disagreement with earlier measurements by Taub and Spaepen on the same alloy (5). In this paper we report new measurements that reconcile the earlier observations by demonstrating the importance of the pre-annealing temperature for the iso-configurational behavior.

Experiments and Results

The samples used in the experiments were disk-quenched Pd_{77.5}Cu₆Si_{16.5} ribbons, 13 μ m thick and 0.22 mm wide. T_g for this alloy was measured to be 645K by differential scanning calorimetry. The viscosity measurements were made using a tensile creep apparatus as described earlier (6). The highest equivalent shear stress used in the experiments was well below the 300 MPa limit for Newtonian flow determined by Taub (7) for Pd₈₂Si₁₈.

Structural Relaxation Experiments. Figure 1 shows the viscosity increase for an as-quenched sample during isothermal annealing at 615K. The viscosity increase is clearly non-linear, with η first decreasing due to the approach to equilibrium, and later increasing due to the onset of rapid crystallization. The portion of the viscosity curve with negligible crystallization was fitted to both unimolecular and bimolecular kinetic models, as explained below.

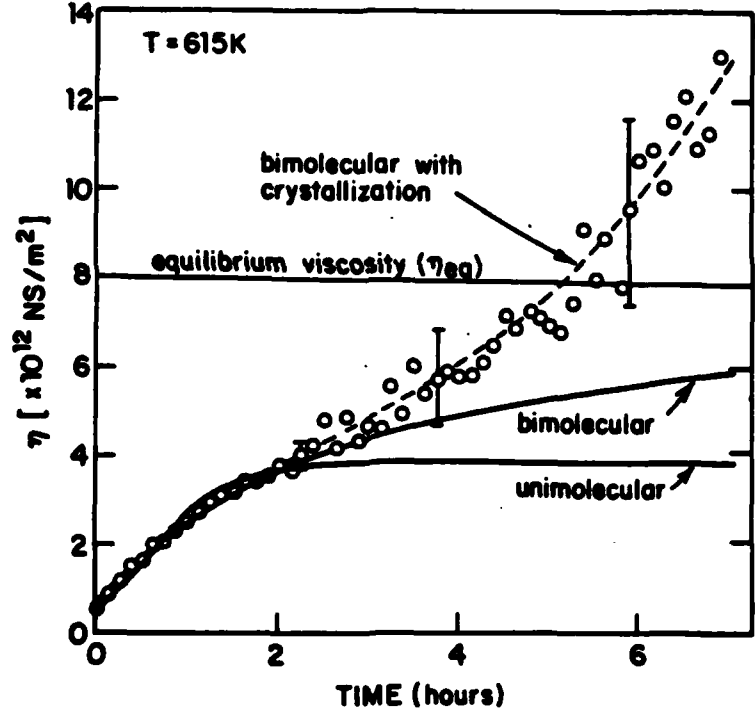


Figure 1 - Example of the non-linear viscosity change with time observed during isothermal annealing of Pd_{77.5}Cu₆Si_{16.5} near the glass transition temperature. The circles are the data points; the lines correspond to the fits by different phenomenological relaxation models.

Since the viscosity is inversely proportional to the concentration of flow defects, n_f , (8) the observed viscosity increase must correspond to a decrease in n_f . Since the system in equilibrium has a finite viscosity, η_{eq} , a number of defects, $n_{f,eq}$, must remain after an infinite annealing time. Two kinetic laws in which n_f becomes zero when equilibrium is reached ($n_f = n_{f,eq}$) have been formulated. They are, respectively, first and second order rate equations in the excess number of defects ($n_f - n_{f,eq}$). For the unimolecular model:

$$\frac{d(n_f - n_{f,eq})}{dt} = -k_1 (n_f - n_{f,eq}) \quad (1)$$

and for the bimolecular model,

$$\frac{d(n_f - n_{f,eq})}{dt} = -k_2 (n_f - n_{f,eq})^2 \quad (2)$$

Integrating equations (1) and (2), gives for the viscosity, respectively:

$$\frac{1}{\eta(t)} = \frac{1}{\eta_{eq}} + \left(\frac{1}{\eta_0} - \frac{1}{\eta_{eq}}\right) \exp(-k_1 t) \quad (3)$$

$$\frac{\eta(t) - \eta_0}{\eta_{eq} - \eta(t)} = \left(\frac{\eta_{eq} - \eta_0}{\eta_{eq}^2} k_2\right) t \quad (4)$$

Three parameters, η_{eq} , k_1 or k_2 , and the initial viscosity η_0 were used in fitting the data. Figure 1 shows the fits obtained from the unimolecular and bimolecular models as light and heavy curves, respectively. Only the first three hours of the creep test were used for fitting. Figure 2 is an enlarged plot of the first three hours of Figure 1. The bimolecular model fits the data very well whereas the unimolecular model does not, due to the fundamental difference in shape between the model curves. Since a quantitative comparison of the quality of the two fits is difficult with the noisy differentiated viscosity curve, the fits were actually performed on the original elongation data. In all our experiments near T_g the χ^2 of the unimolecular fit was larger than that of the bimolecular fit.

Figure 3 shows the fitting parameter η_{eq} , obtained by fitting the data at various temperature to the bimolecular model. Since it is not possible to measure η_{eq} directly due to crystallization, we believe that these values of η_{eq} represent the most reliable measurements of the equilibrium viscosity so far. We have confirmed our values of η_{eq} by observing the isothermal approach to η_{eq} in the reverse direction: a specimen, annealed for a long time at a low temperature, was brought rapidly to a temperature beyond the equilibrium curve and the viscosity *decrease* was observed; a fit through the data before crystallization had the *same* asymptotic value for η_{eq} as the fit to the increasing viscosity. Also shown in figure 3 is a Fulcher-Vogel fit (of the type $\log \eta = A + B/(T - T_0)$) to the η_{eq} values and earlier measurements of the equilibrium viscosity reported by Chen and Goldstein (9) for the same alloy.

It was also possible to describe the viscosity change during crystallization, using an expression first derived by Einstein (10), to calculate the effective viscosity η_{eff} of a medium of viscosity η , containing a small volume fraction, f_c , of rigid particles:

$$\eta_{eff}(t) = \eta(t) (1 + 2.5f_c(t)) \quad (5)$$

By assuming a concentration of crystals n , growing with an interface velocity v , this fraction becomes:

$$f_c = \left(\frac{4\pi}{3} n v^3 \right) t^3 \quad (6)$$

The term in parentheses above is treated as a free parameter, together with the previously found parameters of the bimolecular equation to fit the data. The result is shown as the dashed curve in figure 1. The value of the fitting parameter is in reasonable agreement with direct observations of n , v and f_c .

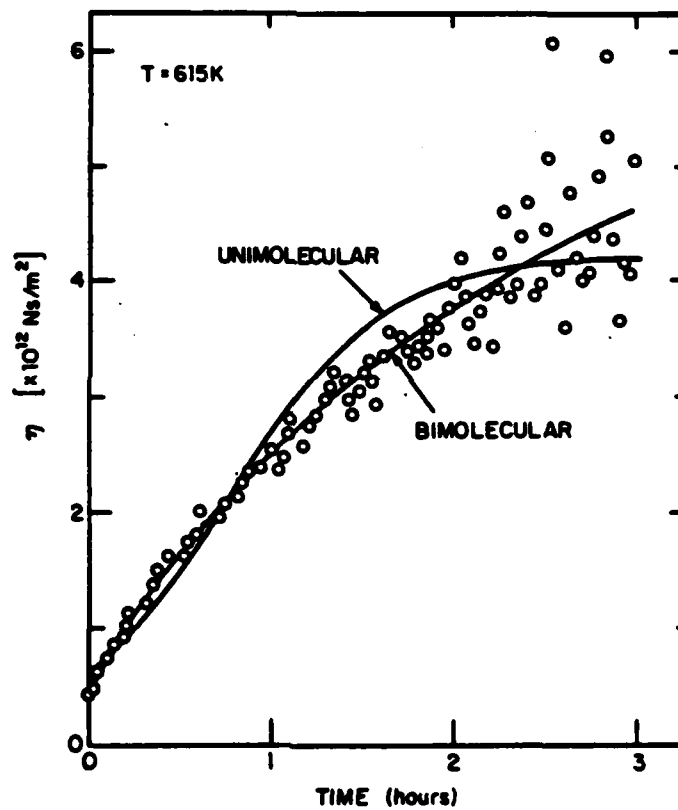


Figure 2 - Enlarged plot of the bimolecular and unimolecular fits to the first three hours of the data in figure 1. The bimolecular model is a better fit to the data (circles) than the unimolecular one. The fundamental difference in shape between the models is clear.

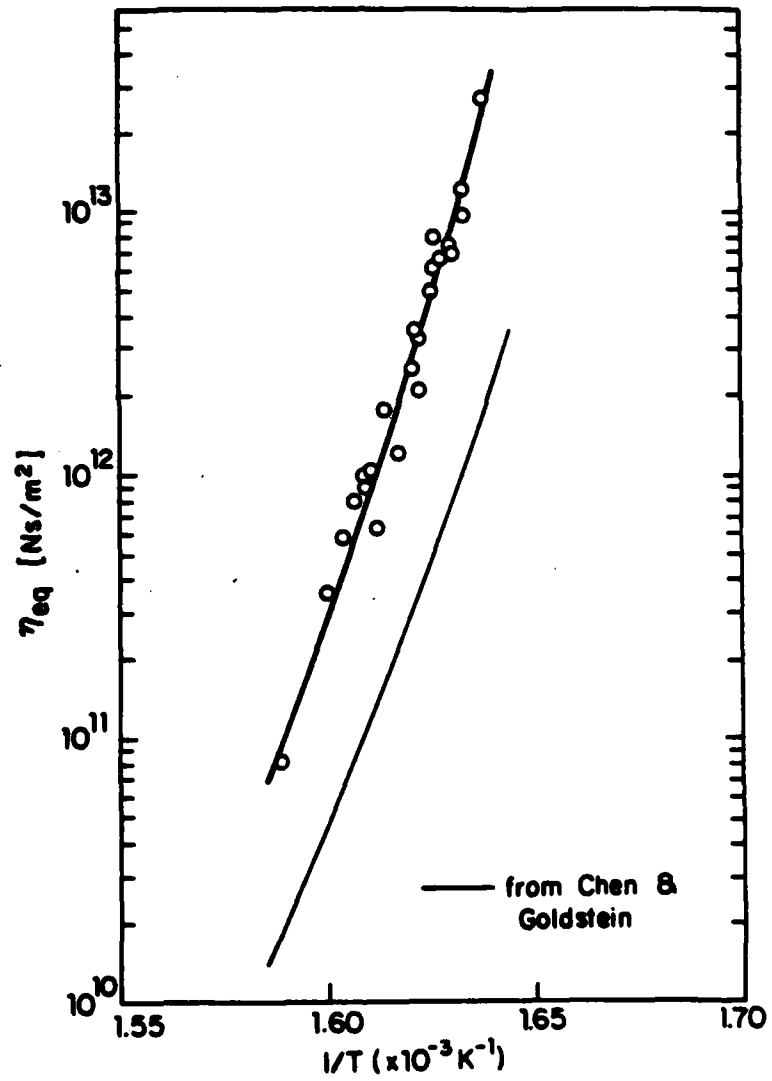


Figure 3 - plot of the temperature dependence of the equilibrium viscosity values, η_{eq} , obtained from the bimolecular fits to a number of relaxation experiments on $\text{Pd-7.5Cu}_6\text{Si}_{16.5}$. Also shown are a Fulcher-Vogel fit through the points, and the earlier results of Chen and Goldstein (9) for the same alloy.

Isoconfigurational Flow Experiments. The results of iso-configurational tests, described above, on the two PdCuSi ribbon samples are summarized in Figure 4. The numbers indicate the order of the measurements. The filled-in circles are for an as-quenched sample first relaxed under load at 529K for 600 hours. Point 1 shows the final viscosity. Points 5-19 trace out an isoconfigurational curve as demonstrated by cycling the temperature and reproducing the measurements. The light dashed line is a likely extension of this curve to include point 4. For the points 5-19, the equivalent shear stress, τ , was 100 MPa. The open circles are previously reported results for an as-quenched sample first relaxed under load at 592K for 48 hours (4). Points 1-11 trace out a first isoconfigurational curve. Except for point 11 which was measured with $\tau = 94$ MPa, and points 12, 14, 15 which were measured with $\tau = 83$ MPa, the rest of the points were measured with $\tau < 52$ MPa. For comparison, figure 4 also shows the isoconfigurational data measured by Taub and Spaepen (4) for a PdCuSi wire sample, annealed for varying lengths of time at temperatures between 500 and 552 K.

Discussion

Structural Relaxation. The bimolecular model, which is the best phenomenological description of viscosity relaxation in the PdCuSi glass has also been shown to describe the viscosity increase during relaxation in amorphous covalently bound systems, such as soda-lime glass (11,12). In these systems, which are modeled as continuous random networks, the flow defects are easily identified as broken bonds, which allow local shear rearrangements. Since annihilation of these bonds occurs when two of them come together to reform a covalent bond, the bimolecular kinetic law of equation (2) is obviously the one that is expected to apply here.

For the metallic glass systems, however, the specific nature of the flow and relaxation events is much less clear, and the nature of the microscopic mechanism that accounts for the bimolecular relaxation kinetics can only be speculated about. For example, it is possible to construct a direct equivalent to the broken bond argument in covalent systems, based on the strong degree of chemical short range order in metal-metalloid (X) glasses, such as PdCuSi. The diffraction evidence shows that the metalloid (X) atoms are ideally surrounded by metal (M) atoms only. If chemical defects, i.e.: X-X neighbors and complementary excess M-M neighbors, can be shown to govern flow, the analogy with the broken covalent bonds would be complete.

It is also possible to use purely topological arguments to construct a bimolecular relaxation mechanism. In that case, a flow defect is a cluster of atoms, wherein as a result of a density or "free volume" fluctuation, a shear rearrangement takes place, resulting in a shear strain which is transferred elastically to the specimen boundary. In such a transformation, free volume is conserved. A free volume fluctuation and hence a flow defect can only be eliminated at a special site or "relaxation defect", which is a cluster of atoms, wherein as a result of a free volume fluctuation, atoms rearrange and transfer at least part of this free volume out to the specimen boundary. Any rearrangement with a dilatational component can be such a relaxation defect (8). The rate of disappearance of the flow defects, \dot{n}_f , is therefore proportional to the product of the concentrations of flow and relaxation defects, $n_f n_r$. This kinetic equation reduces to the bimolecular one if n_r can be shown to be proportional to n_f (2). Note that the unimolecular annihilation reaction (eq.(1)) corresponds to a constant concentration of relaxation defects.

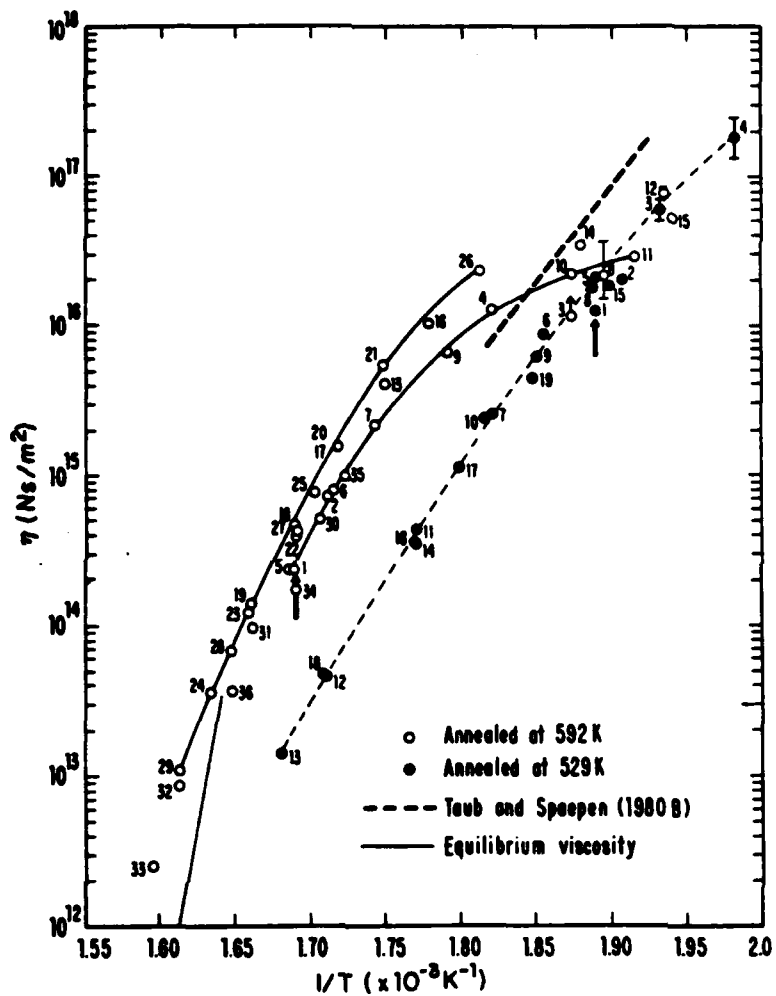


Figure 4 - Isoconfigurational measurements on $\text{Pd}_{77.5}\text{Cu}_6\text{Si}_{16.5}$. The arrows indicate the temperature of annealing prior to the measurement. The dashed line represents earlier measurements by Taub and Spaepen (5). The light solid line is the equilibrium viscosity from Figure 3.

Concerning the equilibrium viscosity, we note that our values for η_{eq} are almost an order of magnitude higher than those measured by Chen and Goldstein (9) for the same alloy. In fact, even without extrapolation to η_{eq} , we measured viscosities greater than those reported by Chen and Goldstein for η_{eq} . We believe that the discrepancy is due to insufficient relaxation in the earlier experiments.

Isoconfigurational Flow. The results of figure 4, show clearly that the isoconfigurational viscosity behavior is very dependent on the configuration of the sample prior to the measurements. Over the temperature range 592 - 582K, the sample annealed at the higher temperature showed a much greater deviation from an Arrhenian temperature dependence than the sample annealed at the lower temperature. Our data for the latter sample are in excellent agreement with the data obtained by Taub and Spaepen (5) for a wire specimen annealed under similar conditions. They reported an activation energy of $240 \pm$ kJ/mole over the temperature range of measurement. A linear fit to points 5-10 gives an activation energy of $246 \pm$ kJ/mole.

In a previous paper (4) we outlined a possible explanation for the non-Arrhenian temperature dependence of isoconfigurational flow. We suggested that the reversible viscosity changes upon cycling of the temperature can be accounted for by fast reversible atom movements which partially redistribute the free volume changes due to thermal expansion. The apparent crossover of the two isoconfiguration curves resulting from differently annealed specimens implies that the isoconfiguration viscosity cannot be a function of only a single structural parameter, such as the average free volume in the sample, but that a second parameter such as the shape of the free volume (non-equilibrium) distribution curve must be taken into account.

The high temperature measurements for the sample annealed at 592K are of special interest in that they are consistent with the new η_{eq} values we report here. Note that point 29 is above the proposed equilibrium viscosity curve, which means that structural relaxation at this temperature leads to a viscosity decrease, i.e., creation of more flow defects. Indeed, when the sample was returned to a lower temperature, at point 30, the measured viscosity was almost a factor of two lower than the iso-configuration line. At the time we reported this result(4) we had not yet determined the new equilibrium viscosity line, and this behavior was simply attributed to the necking of the specimen which eventually led to specimen fracture. In hindsight, necking probably did not start until further heating from point 36 to \sim 633K (the viscosity drop is also rather large to be accounted for by necking), and that the drop in viscosity past point 29 is due to structural relaxation in the opposite sense.

Conclusion

At temperatures near T_g , a non-linear viscosity increase with time is observed during isothermal annealing of as-quenched PdCuSi which can be described well by a bimolecular phenomenological relaxation mode. The equilibrium viscosity values obtained by fitting the data to the bimolecular kinetic equation are almost an order of magnitude higher than the literature data for the same alloy. Using the bimolecular law for the change in viscosity of the amorphous material and treating the volume fraction of crystals as a free parameter in Einstein's expression for the viscosity of a medium with a small volume fraction of rigid particles, we could also account for the viscosity change during crystallization.

Isoconfigurational results on two specimens, annealed at different temperatures prior to the measurements, show the importance of the initial configurations.

Acknowledgements

We thank K.P. Kelton for the use of his fitting program. This work has been supported by the Office of Naval Research, Contract N-000-14-77-C-0002.

References

1. A.I. Taub and F. Spaepen, Acta Met., 28 (1980) p. 1781.
2. A.L. Greer and F. Spaepen, "Creep, Diffusion and Structural Relaxation in Metallic Glasses", pp. 218-239 in Structure and Mobility in Molecular and Atomic Glasses, James M. O'Reilly and Martin Goldstein, eds.; The New York Academy of Sciences, New York, NY, 1981.
3. H.S. Chen and D. Turnbull, J. Chem. Phys., 48 (1968) p. 2560.
4. S.S. Tsao and F. Spaepen, 4th Int. Conf. on Rapidly Quenched Materials (Sendai, 1981).
5. A.I. Taub and F. Spaepen, Scripta Met., 14 (1980) p. 1197.
6. A.I. Taub and F. Spaepen, Scripta Met., 13 (1979) p. 195.
7. A.I. Taub, Acta Met., 28 (1980) p. 633.
8. F. Spaepen, in "Physics of Defects", ed. by R. Balian, J.P. Poirier and M. Kleman, Les Houches Lectures XXXV, North Holland (1981) p. 136.
9. H.S. Chen and M. Goldstein, J. Appl. Phys., 43 (1971) p. 174.
10. A. Einstein, Ann. Phys., 19 (1906) p. 289.
11. H.R. Lillie, J. Amer. Ceram. Soc., 16 (1933) p. 619.
12. G.J. Roberts and J.P. Roberts, 7th Int. Conf. on Glass (Brussels, 1969).

COMPOSITIONALLY MODULATED METALLIC GLASSES

A. L. GREER

Div. of Applied Sciences, Harvard University, Cambridge, MA 02138, U.S.A.

1. INTRODUCTION

Metallic glasses (amorphous alloys) are of considerable scientific and technological interest (reviewed in, e.g., [1]). They were first produced by rapid quenching of the melt [2], but other techniques can be used, including deposition by evaporation or sputtering. Alloys which have been produced in glassy form fall into two main categories: noble or transition metals with 15-25 atomic % of metalloids; and combinations of early and late transition metals, which typically form glasses over wider composition ranges.

Diffusion measurements in metallic glasses have to be made below the glass transition temperature, T_g , in order to avoid rapid crystallization, and the diffusivities are consequently very low ($<10^{-20} \text{m}^2 \text{s}^{-1}$). Such diffusivities have been estimated by diffusing a species in from the specimen surface and measuring the composition profile using sputter sectioning or Rutherford backscattering [3]. While these techniques are useful, much lower diffusivities can be determined by X-ray measurement of the interdiffusion in compositionally modulated thin films, a technique first used by DuMond and Youtz [4], and developed by Cook and Hilliard [5]. As-produced metallic glasses can lower their free energy not only by crystallizing but also by relaxing their glassy structure. It is important to take this into account in interpreting diffusion measurements. The structural relaxation is accompanied by a slight densification ($\lesssim 0.4\%$) and by a marked reduction in atomic mobility. The modulated film technique can be used to monitor the diffusivity continuously. The composition-profiling techniques, on the other hand, can measure the diffusivity only after long anneals, during which substantial relaxation also occurs.

The ability to make time-resolved measurements of very low diffusivities makes the use of compositionally modulated thin films especially valuable in studying metallic glasses. The analysis of interdiffusion measurements is outlined in Section 2, and in Section 3 the experimental results to date are reviewed. Possibilities for further work on metallic glasses are described in Section 4.

2. INTERDIFFUSION IN MODULATED AMORPHOUS ALLOYS

In an amorphous material a composition modulation gives rise to satellites about the (000) X-ray reflection. The intensity of the first-order satellite is proportional to the square of the amplitude of the first Fourier component of the modulation. In a linear analysis the Fourier components are considered independent, and the effective interdiffusivity, \bar{D}_λ , is given by the decay rate of the first-order satellite intensity, $I(t)$,

$$\bar{D}_\lambda = - \frac{\lambda^2}{8\pi^2} \frac{d}{dt} \ln [I(t)/I_0] \quad (1)$$

where I_0 is the initial intensity and λ is the modulation wavelength [4]. \bar{D}_λ is dependent on the modulation wavelength. For crystalline materials, an analysis based on discrete atomic planes is necessary [6]. For amorphous materials, however, a continuum analysis, first developed by Cahn and Hilliard [7], is more appropriate. In their analysis, for a binary solid solu-

tion, \bar{D}_λ is related to the macroscopic interdiffusion coefficient, \bar{D} , by

$$\bar{D}_\lambda = \bar{D} \left[1 + \frac{8\pi^2 \kappa}{f''_0 \lambda^2} \right], \quad (2)$$

where f''_0 is the second derivative, with respect to composition, of the Helmholtz free energy per unit volume of the homogeneous phase, and κ is the gradient energy coefficient. Assuming only nearest neighbor interactions in a regular solution, κ is given by

$$\kappa = \frac{2\Delta H r_0^2}{3V}, \quad (3)$$

where ΔH is the heat of mixing per mole at the equiatomic composition, r_0 is the interatomic distance, and V is the molar volume. With the same assumptions f''_0 is found to be:

$$f''_0 = \frac{-4}{V} [2\Delta H - RT], \quad (4)$$

where R is the gas constant. Given adequate thermodynamic data, f''_0 would be known, and it would be possible to test eq. (3) directly. For novel, glass-forming compositions such data are often not available, and would be difficult to obtain at the temperatures of interest because of the metastability of metallic glasses.

3. SURVEY OF RESULTS

In this section the work on compositionally modulated metallic glasses will be reviewed. This work has been carried out at Harvard University. Compositionally modulated films were produced by DC sputtering from two targets of different compositions. Experimental details are given elsewhere [8,9].

Preliminary Measurements

The first compositionally modulated metallic glasses were made by Rosenblum et al. [8,9]. The films, of composition $(\text{Pd}_{80}\text{Au}_7\text{Si}_{13})_{70}/\text{Fe}_{30}$, showed only a first-order X-ray satellite, indicating a roughly sinusoidal composition modulation. On annealing, the satellite intensities decayed, and using eq. (1), \bar{D}_λ was derived. It was found that \bar{D}_λ decreased with annealing time, rapidly at first, and then tended to stabilize. This behavior was attributed to structural relaxation. Because of problems with crystallization, new films, of composition $(\text{Pd}_{85}\text{Si}_{15})_{61}/(\text{Fe}_{85}\text{B}_{15})_{39}$, were produced, in which each type of layer was of glass-forming composition. Interdiffusion measurements on these films confirmed the earlier results.

Greer et al. [10,11] made measurements on films of composition $(\text{Pd}_{85}\text{Si}_{15})_{50}/(\text{Fe}_{85}\text{B}_{15})_{50}$, and the remainder of the results quoted in this paper will be from their work. Films with a total thickness of $\sim 5\mu\text{m}$ and modulation wavelengths of 2.2\AA to 74.6\AA were produced. Only a weak first-order satellite was observed for the smallest wavelength film, while for the $\lambda = 74.6\text{\AA}$ film peaks out to fourth order were detected. The metals dominate the X-ray scattering, and the measured \bar{D}_λ is the Pd-Fe interdiffusivity. Although the composition of the films is complex, the results are analyzed according to the treatment for a binary system, as outlined in Section 2.

Gradient Energy Effects

Two films, with $\lambda = 20.6\text{\AA}$ and 39.4\AA , were annealed at 250°C . The behavior of the first-order satellite intensities is shown in Fig. 1. For

each film there is a rapid initial drop in intensity, the origins of which are considered in the next section. After ~ 15 hours, however, $\ln(I(t)/I_0)$ falls linearly with time, indicating a constant interdiffusivity and a negligible rate of structural relaxation in the films. Since the annealing temperature was the same in each case, the degree of relaxation at a given time is the same in each film. From the final gradients of the plots, \bar{D}_λ was calculated using eq. (1) and was found to be: $7.09 \times 10^{-26} \text{m}^2 \text{s}^{-1}$ for the $\lambda = 20.6\text{\AA}$ film; and $1.37 \times 10^{-24} \text{m}^2 \text{s}^{-1}$ for the $\lambda = 39.4\text{\AA}$ film. The difference in these values is a manifestation of gradient energy effects. Analyzing these effects according to eq. (2), it is found that $\bar{D} = 1.86 \times 10^{-24} \text{m}^2 \text{s}^{-1}$ and that $\kappa/f_0'' = -5.18 \times 10^{20} \text{m}^2$. Since \bar{D} is positive, f_0'' is positive, and κ must be negative. Negative values of the gradient energy coefficient are expected for ordering systems. Although no directly relevant thermodynamic data are available, ordering might be expected from the behavior of Pd-Fe solid solutions. Using eqs. (3) and (4), the heat of mixing, ΔH , at 250°C is estimated to be $+2.45 \text{kJ mol}^{-1}$.

Figure 2 is a plot of \bar{D}_λ vs λ , calculated from eq. (2) and fitted to the measured interdiffusivities. The negative values of \bar{D}_λ indicate phase-separation at low wavelength, i.e. ordering. Experimental evidence for this will be considered later. The critical wavelength, λ_c , for which \bar{D}_λ is zero, is 20.22\AA , a value which is unusually large compared to typical crystalline systems [5]. In earlier work [10] it was assumed that for $\lambda > 20\text{\AA}$, gradient energy effects could be ignored. Clearly this is not the case in this system.

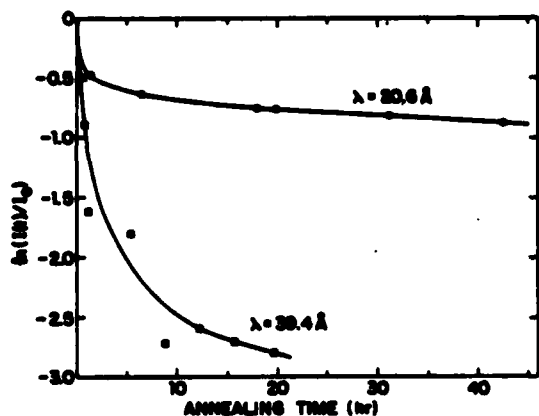


Fig. 1. Decay of first-order satellite intensities from films with $\lambda = 20.6\text{\AA}$ and $\lambda = 39.4\text{\AA}$ on annealing at 250°C .

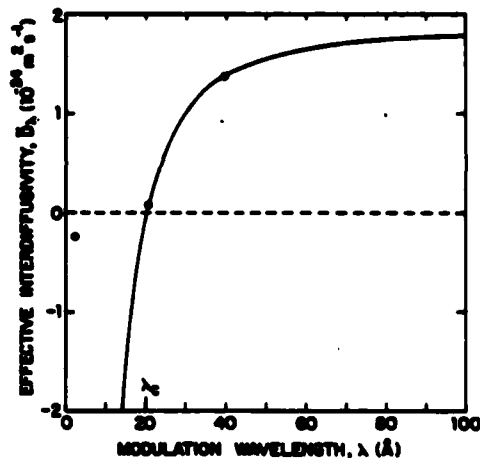


Fig. 2. \bar{D}_λ vs λ calculated according to eq. (2) and fitted to the measurements at $\lambda = 20.6\text{\AA}$ and $\lambda = 39.4\text{\AA}$.

Structural Relaxation

The initial non-linear decay in satellite intensity, shown in Fig. 1, could be due to a number of causes. \bar{D} is composition-dependent, and with a large initial modulation amplitude this could give rise to non-linear effects. The calculations of DeFontaine [12], however, suggest that such effects should be small. There is small angle X-ray scattering from the films which decays in about 2 hours at 250°C . This may arise from changes in the films such as elimination of voids or reduction of argon content, which could have an effect on the very early stages of interdiffusion. The continuing decrease in \bar{D}_λ after ~ 2 hours is unlikely to be due to either of the above causes and is attributed to structural relaxation. A film with $\lambda = 32.2\text{\AA}$ was annealed at 300°C in order to study the relaxation kinetics. The behavior of the first- and second-order satellite intensities is shown in

Fig. 3. The complex behavior of the second-order satellite is believed to arise from the composition dependence of \bar{D} [12,13], and the form of the curve is in qualitative agreement with the results of Tsakalakos [13] on crystalline Cu-Ni films. The first-order satellite was used to determine \bar{D}_λ , and \bar{D} was calculated using the value of κ/f_0^n derived above. It was found that $1/\bar{D}$ rose linearly with time (Fig. 4). The low value of \bar{D} after 150 minutes is believed to be due to the onset of crystallization.

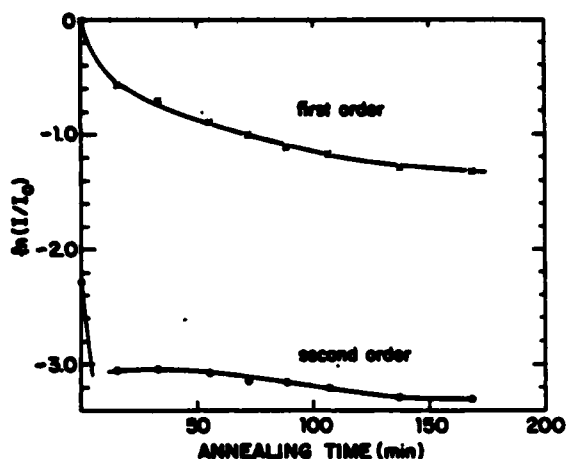


Fig. 3. Decay of satellite intensities on annealing of a $\lambda = 32.2\text{\AA}$ film at 300°C .

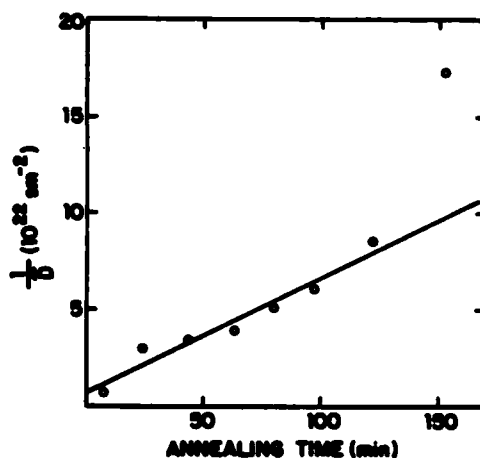


Fig. 4. Relaxation kinetics of $1/\bar{D}$ in $\lambda = 32.2\text{\AA}$ film annealed at 300°C .

It is evident that structural relaxation has a large effect on \bar{D} . In order to obtain a physically meaningful activation energy for \bar{D} it is essential that the experiment be carried out under isoconfigurational conditions. This can be done conveniently and accurately using a single modulated film. As can be seen from Fig. 1, after the $\lambda = 20.6\text{\AA}$ sample had been held at 250°C for ~ 40 hours the changes in \bar{D}_λ were undetectable (although the sample was not in configurational equilibrium). The temperature was then lowered to 230°C , \bar{D}_λ was measured at that temperature, and on returning to 250°C it was verified that \bar{D}_λ at 250°C was unchanged; i.e. that no further relaxation had taken place. This procedure was repeated for excursions to 220°C , 210°C and 270°C . As shown in Fig. 5, the temperature dependence of \bar{D} is Arrhenius-type, with an isoconfigurational activation energy of $195 \pm 15\text{kJ mol}^{-1}$. The value of the pre-exponential factor, $5.6 \times 10^{-5}\text{m}^2\text{s}^{-1}$, is reasonable.

In understanding atomic transport in metallic glasses it is important to study the relationship between the diffusivity, D , and the viscosity, η . For liquid metals, experimental results are in fair agreement ($\pm 50\%$) with the Stokes-Einstein relation:

$$D = kT/6\pi\eta r, \quad (5)$$

where k is Boltzmann's constant, T is the temperature and r is an average ionic radius. In metal-metalloid glasses, as in the present case, it is expected that the metal atom diffusivity would be related to η . The viscosity data of Taub and Spaepen [14] on $\text{Pd}_{82}\text{Si}_{18}$ glass were chosen for comparison. The viscosity was measured over the range 151°C to 264°C and exhibited an activation energy of $192 \pm 17\text{kJ mol}^{-1}$, very close to the value for interdiffusion (Fig. 5). At all temperatures structural relaxation caused η to rise linearly with annealing time. Fig. 4 shows similar behavior for $1/\bar{D}$. By comparing the rates of increase, D and η can be related, without concern about the degree of relaxation. At 300°C , $d\eta/dt = 1.04 \times 10^{10}\text{Nm}^{-2}$ (extrapolated) and $d(1/\bar{D})/dt = 1.01 \times 10^{19}\text{m}^{-2}$. From these values it is calculated

that \bar{D} is about 160 times the value that would be estimated from η using eq. (5). Thus, although \bar{D} and η are closely related, showing the same activation energy and relaxation behavior, there are diffusional jumps that do not lead to viscous flow. The Stokes-Einstein relation is not valid in these glasses.

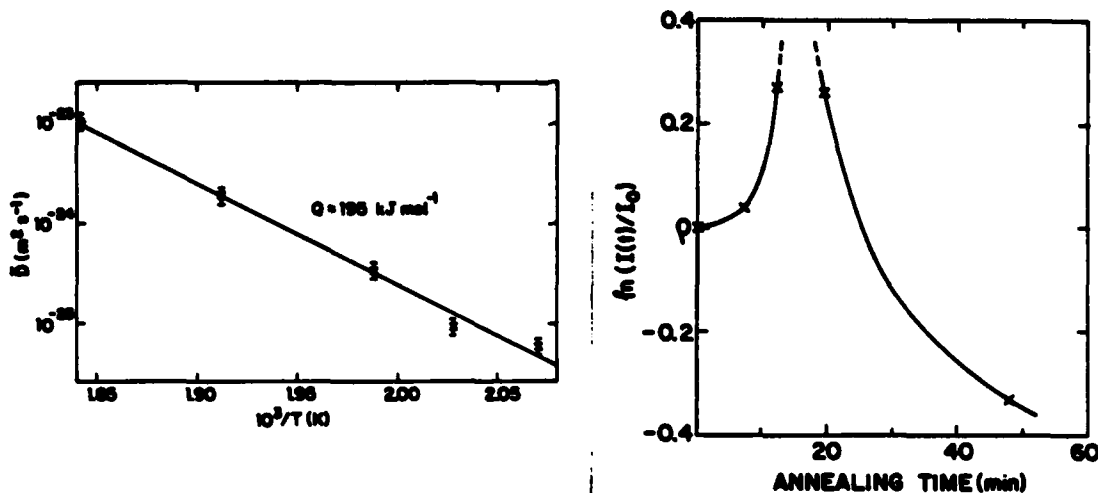


Fig. 5. The temperature dependence of \bar{D} in a $\lambda = 20.6\text{\AA}$ film, indicating order satellite intensity from a the isoconfigurational activation energy. $Q = 195 \text{ kJ mol}^{-1}$. Fig. 6. The behavior of the first-order satellite intensity from a $\lambda = 2.275\text{\AA}$ film annealed at 250°C .

Interdiffusion at Very Short Wavelength

An interesting feature of amorphous materials is that it is possible for the wavelength of a composition modulation to be less than the interatomic spacing. In a crystal this would be possible only if the layers were high-index atomic planes. The Pd-Fe interatomic distance is estimated to be $\sim 2.65\text{\AA}$, and a Pd-Si/Fe-B modulated film was produced with $\lambda = 2.275\text{\AA}$. The behavior of the first-order satellite intensity on annealing at 250°C is shown in Fig. 6. The initial rise in intensity is expected in ordering systems at short wavelength. An approximate value of \bar{D} is plotted in Fig. 2; the value does not lie close to the curve, but eq. (2) is expected to break down at very short wavelength. The subsequent drop in intensity is attributed to ordering within the layers. This removes the one-dimensional order and homogenizes the film.

Discussion

The values of interdiffusivity determined above are in good agreement with metal atom diffusivities in metallic glasses determined by composition profiling. In previous work [10], the values from modulated films appeared somewhat low because gradient energy effects were not taken into account. The values of \bar{D} determined in metallic glass films are greater than the values expected for single crystal films at the same temperature, but smaller than the values expected for fine-grained films. In the work described above, the lowest measured \bar{D}_λ was $1.31 \times 10^{-27} \text{ m}^2 \text{ s}^{-1}$. If this \bar{D}_λ were to be measured by composition profiling, an anneal of over 200 years would be required for the necessary penetration distance of 30\AA .

4. PROSPECTS FOR FURTHER WORK

Not only are modulated films useful in studying metallic glasses, but the use of glasses in the films is useful in studying the effects of compo-

sition modulation. Some current research directions are indicated below.

Studies of Metallic Glasses

Interdiffusion studies on a wider range of metallic glass systems would provide valuable information on the stability and thermodynamics of non-crystalline phases. The use of films containing only two elements (possible in binary systems with a wide glass-forming range) would simplify the interpretation of results. Some metallic glasses phase-separate, and it would be interesting to study these systems in the same manner as that used by Tsakalakos for crystalline Cu-Ni films [15].

Studies of Composition Modulation Effects

The major advantages of using amorphous alloys, instead of crystalline ones, to study these effects are:

(i) The modulation wavelength can be adjusted continuously, whereas in crystalline materials effects due to interference with the crystal periodicity can occur.

(ii) Coherency strains are avoided, and the absence of internal strains greatly simplifies the interpretation of certain effects, such as the dependence of \bar{D}_λ and elastic modulus on modulation wavelength.

(iii) In amorphous alloys the composition can be adjusted continuously, often over a wide range. This is not possible in crystalline materials because of the formation of stoichiometric compounds.

ACKNOWLEDGEMENTS

This work was supported by the Office of Naval Research under contract N00014-77-C-0002 and by the National Science Foundation under contract DMR80-20247.

REFERENCES

1. R.W. Cahn, *Contemp. Phys.* 21, 43 (1980).
2. P. Duwez, R.H. Willens and W. Klement, *Nature* 187, 869 (1960).
3. M. Kijek, M. Ahmadzadeh, B. Cantor and R.W. Cahn, *Scripta Metall.* 14, 1337 (1980).
4. J. DuMond and J.P. Youtz, *J. Appl. Phys.* 11, 357 (1940).
5. H.E. Cook and J.E. Hilliard, *J. Appl. Phys.* 40, 2191 (1969).
6. H.E. Cook, D. DeFontaine and J.E. Hilliard, *Acta Metall.* 17, 765 (1969).
7. J.W. Cahn and J.E. Hilliard, *J. Chem. Phys.* 28, 258 (1958).
8. M.P. Rosenblum, F. Spaepen and D. Turnbull, *Appl. Phys. Lett.* 37, 184 (1980).
9. M.P. Rosenblum, Ph.D. Thesis, Harvard University (1979).
10. A.L. Greer, C.-J. Lin and F. Spaepen, *Proc. 4th Int. Conf. on Rapidly Quenched Metals* (eds. T. Masumoto and K. Suzuki). Japan Institute of Metals (1982).
11. R.C. Cammarata and A.L. Greer, to be published.
12. D. DeFontaine, Ph.D. Thesis, Northwestern University (1967).
13. T. Tsakalakos, Ph.D. Thesis, Northwestern University (1977).
14. A.I. Taub and F. Spaepen, *Acta Metall.* 28, 1781 (1980).
15. T. Tsakalakos, *Scripta Metall.* 15, 235 (1981).

INTERDIFFUSION STUDIES IN METALLIC GLASSES USING COMPOSITIONALLY MODULATED THIN FILMS

R.C. CAMMARATA and A.L. GREER

Division of Applied Sciences, Harvard University, Cambridge, Massachusetts 02138, U.S.A.

Interdiffusivities are measured in compositionally modulated amorphous thin films as a function of modulation wavelength. The sensitivity of this method is demonstrated by the measurement of very low interdiffusivities, and permits the observation of structural relaxation effects. From these results we are able to determine the general thermodynamic behavior of the alloy system, and to derive the bulk interdiffusivity. Our data suggest that, contrary to earlier reports, the Stokes-Einstein equation (relating diffusivity and viscosity) is not valid in metallic glasses.

1. INTRODUCTION

Two major difficulties arise when making diffusion measurements in metallic glasses. The first is that the experiments must be performed below the glass transition temperature T_g in order to avoid crystallization. Consequently, the diffusivities tend to be rather low ($< 10^{-20} \text{ m}^2 \text{ s}^{-1}$). The second difficulty is that structural relaxation may occur, and this should be taken into account. In order to derive a physically meaningful activation energy for diffusion, it is necessary to make measurements on samples with the same degree of relaxation.

In this work interdiffusivities were obtained from X-ray measurements of the decay in amplitude of a composition modulation in a thin film. Time-resolved measurements of very low diffusivities are possible with this technique. This allows the monitoring of structural relaxation. In addition, it is possible to determine an activation energy for diffusion from isoconfigurational measurements in one sample at different temperatures.

In this paper, which extends the earlier work of Greer, et al.¹ we have investigated the dependence of the interdiffusivity in compositionally modulated amorphous thin films on the modulation wavelength. Some features of atomic transport in metallic glasses, inferred from these results, necessitate a revision of the conclusions presented in the previous work.

2. EXPERIMENTAL METHODS

The measurement of interdiffusivities through the use of compositionally modulated thin films was first suggested by Dumond and Youtz,² and developed

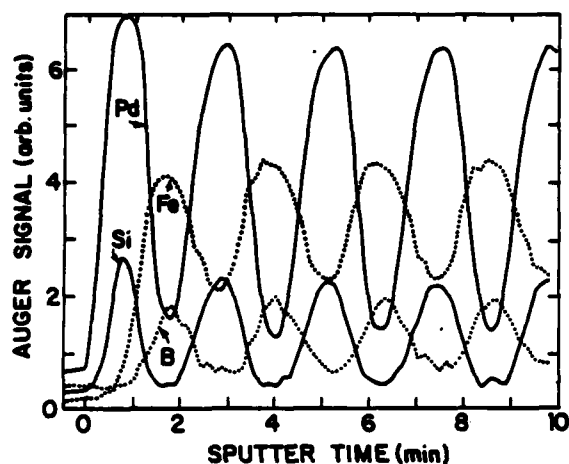


FIGURE 1
Composition variation in an as-produced compositionally modulated thin film ($\lambda = 68.8\text{\AA}$), measured by Auger spectroscopy.

for epitaxial crystalline films by Cook and Hilliard.³ This technique was first applied to amorphous systems by Rosenblum, et al.⁴

In this study, compositionally modulated amorphous films of $(\text{Pd}_{85}\text{Si}_{15})_{50}/(\text{Fe}_{85}\text{B}_{15})_{50}$ were produced by DC sputtering. Figure 1 shows the composition variation of an as-deposited film of modulation wavelength $\lambda = 68.8\text{\AA}$. This profile was obtained by Auger electron spectroscopy, which continuously measured the composition of the film surface as it was being ion milled.

The figure shows that the film contains a definite periodicity in composition variation. (Determination of the modulation wavelength, by X-ray measurements, can be used to calibrate the ion milling rate.) Since ion milling rates and the Auger electron escape depths can vary for each element, and since the bottom of the milled area may not be parallel with the layers; any detailed conclusions drawn from the figure are unreliable.

In an amorphous film, the composition modulation gives rise to X-ray satellites about the (000) reflection, which correspond to the Fourier modes of the modulation. When the composition amplitudes are small, the various modes behave independently during annealing. The effective interdiffusivity \tilde{D}_λ , as a function of λ , is obtainable from the rate of decay of the intensity $I(t)$ of the first-order satellite²

$$\tilde{D}_\lambda = -(\lambda^2 \ln[I(t_2)/I(t_1)]) / 8\pi^2(t_2 - t_1) \quad (1)$$

The complete experimental details of the preparation, annealing, and X-ray measurements of the modulated thin films can be found elsewhere.^{1,4}

3. THEORY

According to the Cahn-Hilliard theory of compositionally inhomogeneous systems,⁵ \tilde{D}_λ , for binary alloys, is related to the bulk interdiffusivity \tilde{D} by

$$\tilde{D}_\lambda = \tilde{D}[1 + 8\pi^2 K / f''_0 \lambda^2] \quad (2)$$

where f''_0 is the second derivative, with respect to composition, of the Helmholtz free energy of a homogeneous phase per unit volume and K is a

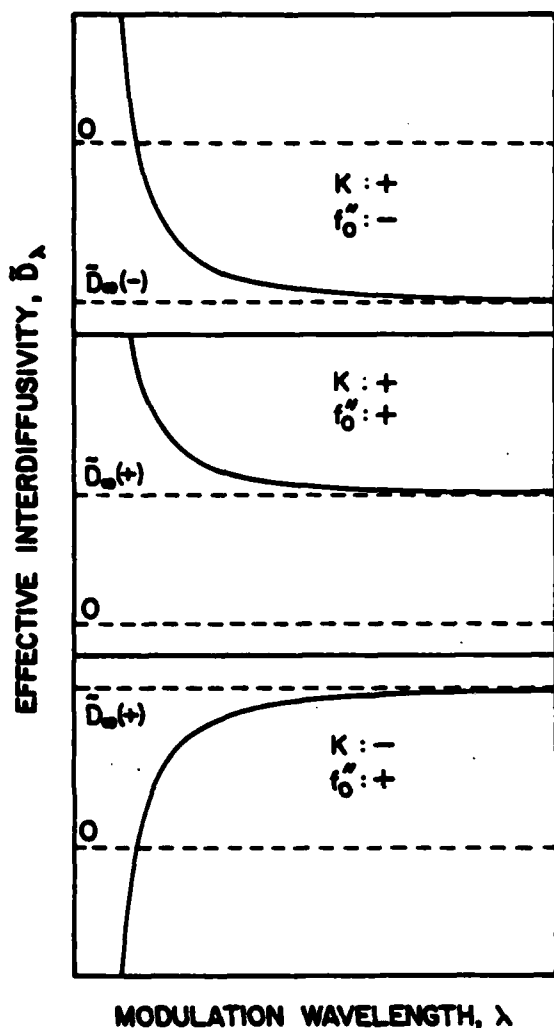


FIGURE 2
Schematic behavior of the effective interdiffusivity \bar{D}_λ as a function of the modulation wavelength λ for the three possible thermodynamic conditions.

ordering systems. As can be seen from Equations (3), in the regular solution model, K and f_0'' cannot be negative simultaneously.

According to the above discussion, by measuring the dependence of \bar{D}_λ on λ in compositionally modulated thin films, the general thermodynamic behavior of the bulk system can be ascertained. Since thermodynamic information on glass forming compositions is scarce and difficult to determine by conventional means at high undercooling, the modulated thin film technique is expected to be quite useful in characterizing the thermodynamic behavior of amorphous alloys.

As was mentioned, the above analysis is valid for binary alloys. In this paper, we will consider our films to be binary Pd-Fe systems. It is hoped that

gradient energy coefficient. These can be evaluated for a regular solution model:⁵

$$\begin{aligned} f_0'' &= 4[RT - 2\Delta U]/V \\ K &= 2\Delta U r^2/3V. \end{aligned} \quad (3)$$

ΔU is the energy of mixing per mole of equiatomic solution, V is the molar volume, R is the gas constant, T is the absolute temperature, and r is the nearest neighbor distance.

Since, from Equations (3), f_0'' and K can be either positive or negative, a variety of possible behavior of \bar{D}_λ with respect to λ can be conceived, as shown schematically in Figure 2. The first curve represents the case when K is positive and f_0'' is negative, conditions under which an unstable homogeneous system can spinodally decompose. When K and f_0'' are both positive, the behavior of \bar{D}_λ is shown by the second curve. For a homogeneous alloy, these conditions describe a stable or metastable phase separating system. The behavior exhibited by the third curve is expected when K is negative and f_0'' is positive, conditions which describe

this has some validity, since they are the predominant species, and would account for almost all the measured X-ray scattering.

4. RESULTS AND DISCUSSION

Interdiffusivities were obtained for four films with modulation wavelengths between 20.6 and 39.4 Å. During the early stages of the anneals (at 250°C) all films displayed a nonlinear decrease of $\ln I(t)$ with respect to time. Most of this initial nonlinearity can be attributed to structural relaxation.⁶ Eventually, all films exhibited linear behavior, and \tilde{D}_λ for each film was calculated using Equation (1). This linear behavior (constant \tilde{D}_λ) implies that each of the films were, during this part of their anneals, in an isoconfigurational state. Presumably, since all the films were produced in the same way and exhibited linear behavior after approximately the same amount of annealing (~ 15 hours), they all had about the same degree of relaxation.

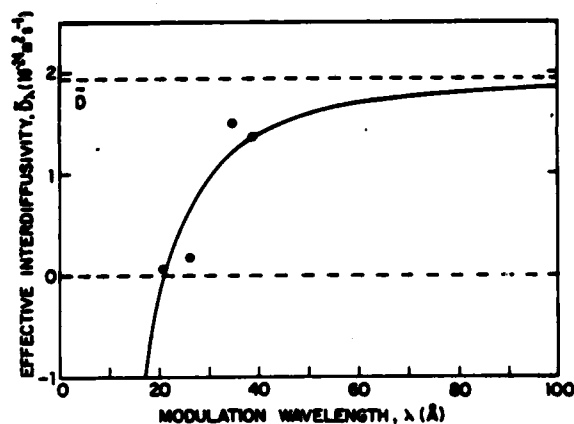


FIGURE 3
The measured interdiffusivity \tilde{D}_λ at 250°C
as a function of the modulation
wavelength λ .

The values of \tilde{D}_λ are plotted in Figure 3. Comparison with Figure 2 shows that amorphous PdSi/FeB behaves as an ordering system. In the crystalline state, there are ordering reactions in the Pd-Fe system.⁷ In the present case, however, the unknown effects of the metalloids preclude any definitive conclusions about the thermodynamic behavior of an amorphous Pd-Fe system.

A linear regression fit of \tilde{D}_λ versus $1/\lambda^2$ was made using Equation (2), and the bulk ($\lambda \rightarrow \infty$) interdiffusivity at 250°C was determined to be $1.94 \times 10^{-24} \text{ m}^2 \text{ s}^{-1}$. The value of the pre-exponential factor (which was determined using the reported¹ activation energy of 195 kJ/mole), $5.6 \times 10^{-5} \text{ m}^2 \text{ s}^{-1}$, appears reasonable. As a comparison, for crystalline systems, the pre-exponential factor is $4.9 \times 10^{-5} \text{ m}^2 \text{ s}^{-1}$ for Fe diffusion in γ -Fe and is $2.1 \times 10^{-5} \text{ m}^2 \text{ s}^{-1}$ for Pd self diffusion.⁸

It has been reported⁹ that in metallic glasses, D is dependent on the atomic radius, a , of the diffusing metal only, and independent of the radii of the atoms comprising the glass. Assuming that D is just a function of this particular atomic radius, the viscosity η , and the temperature, dimensional analysis (see, for example, ¹⁰) leads to the following expression:

$$D = \alpha T / na \quad (4)$$

where α is a proportionality constant. When α is equal to $k/6\pi$, where k is Boltzmann's constant, Equation (4) becomes the Stokes-Einstein equation, which has been shown to be valid to within 50% in some liquid metals when a is taken

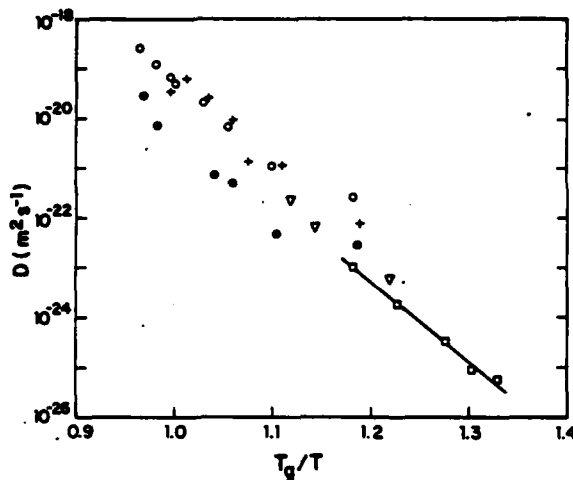


FIGURE 4
Compilation of data on metal diffusion in metal-metalloid glasses.

- Pd-Fe interdiffusion in PdSi/FeB, isoconfigurational measurements, this and previous work.¹
- Au in relaxed Pd_{77.5}Cu₆Si_{16.5} (13)
- Au in relaxed Pd_{77.5}Cu₆Si_{16.5} (14)
- + Au in relaxed Fe₄₀Ni₄₀B₂₀ (14)
- ▽ Au in Pd₈₀Si₂₀ (15)

to be an average ionic radius.¹¹ It had been reported¹ that the Stokes-Einstein equation may also be valid for Pd diffusion in PdSi/FeB metallic glasses. However, an effective interdiffusivity was used, uncorrected for the wavelength dependence. Using the value for \bar{D} determined in this work, and taking¹ $a = 0.72\text{\AA}$, leads to an α in Equation (4) equal to about $31k$ which means that the Stokes-Einstein equation is not valid. This has important implications regarding the nature of atomic transport mechanisms in amorphous metals.¹²

5. COMPARISON WITH OTHER DIFFUSION MEASUREMENTS

In Figure 4, the diffusivity of Au in Pd- and Fe-based metallic glasses measured by various profiling techniques¹³⁻¹⁵ has been plotted along with the diffusion measurements made in this and previous work¹ by the modulated thin film method for the PdSi/FeB system. The temperature axis has been normalized with respect to the glass transition temperature. As can be seen, when plotted in this way, the measurements made by the thin film method are in good agreement with the other data, in both absolute value and activation energy. With the exception of Chen et al.,¹³ in the other work on Au diffusion,^{14,15} no effects of structural relaxation were observed. This is probably due to the lack of sensitivity, relative to the modulated film technique, of the profiling methods used.¹²

6. CONCLUSIONS

We have measured interdiffusivities in metallic glasses through the use of compositionally modulated thin films. This method is very sensitive, allowing the detection of structural relaxation effects and the measurement of low diffusivities ($\geq 10^{-27} \text{m}^2 \text{s}^{-1}$). The interdiffusivities were found to be dependent on the modulation wavelength. From these measurements we were able to classify the PdSi/FeB amorphous alloy as an ordering system, which may have implications concerning compositional short range ordering^{12,16} in metallic glasses. Also a bulk interdiffusivity was determined to be $5.6 \times 10^{-5} \exp(-195 \text{kJmol}^{-1}/RT) \text{m}^2 \text{s}^{-1}$. Based on this value, we have shown that the Stokes-Einstein equation, relating diffusivity to viscosity, is not valid in metallic glasses as has been previously reported.

ACKNOWLEDGEMENTS

The authors thank Prof. F. Spaepen and Mr. C.-J. Lin for many useful discussions, and Mr. F.N. Molea, Mr. J.L. Bell, and Mr. K. Campbell for their technical assistance. This work was supported by the Office of Naval Research under contract N00014-77-C-0002 and by the National Science Foundation under contract DMR80-20247.

REFERENCES

- 1) A.L. Greer, C.-J. Lin, and F. Spaepen, in: Proc. 4th Int. Conf. on Rapidly Quenched Metals, eds. T. Masumoto and K. Suzuki (Japan Inst. of Metals, 1982) pp. 567-572.
- 2) J. Dumond and J.P. Youtz, J. Appl. Phys. 11 (1940) 357.
- 3) H.E. Cook and J.E. Hilliard, J. Appl. Phys. 40 (1969) 2191.
- 4) M.P. Rosenblum, F. Spaepen, and D. Turnbull, Appl. Phys. Lett. 37 (1980) 184.
- 5) J.W. Cahn and J.E. Hilliard, J. Chem. Phys. 28 (1958) 258.
- 6) A.L. Greer, in: Modulated Structure Materials, NATO ASI Series, Applied Sciences, ed. T. Tsakalakos (Martinus Nijhoff, The Hague, 1983) in press.
- 7) M. Hansen, Constitution of Binary Alloys (McGraw-Hill, New York, 1958).
- 8) J. Askill, Tracer Diffusion Data for Metals, Alloys, and Simple Oxides (Plenum Press, New York, 1970).
- 9) B. Cantor and R.W. Cahn, in: Amorphous Metallic Alloys, ed. F.E. Luborsky (Butterworths, London, 1983) pp. 487-505.
- 10) A.H. Cottrell, Mechanical Properties of Matter (John Wiley and Sons, New York, 1964).
- 11) N.H. Nachtrieb, in: Liquid Metals and Solidification (ASM, Cleveland, Ohio, 1958) p. 49.
- 12) A.L. Greer, this volume.
- 13) H.S. Chen, L.C. Kimerling, J.P. Poate, and W.L. Brown, Appl. Phys. Lett. 32 (1978) 461.
- 14) D. Akhtar, B. Cantor, and R.W. Cahn, Acta Metall. 30 (1982) 1571.
- 15) P. Gupta, K.N. Tu, and K.W. Asai, Thin Solid Films 90 (1982) 131.
- 16) T. Egami, Mater. Res. Bull. 13 (1978) 557.

ATOMIC TRANSPORT AND STRUCTURAL RELAXATION IN METALLIC GLASSES

A.L. GREER

Division of Applied Sciences, Harvard University, Cambridge, Massachusetts 02138, U.S.A.

Structural relaxation effects in metal-metalloid glasses are reviewed. Data on viscous flow and atomic diffusion are presented, and possible mechanisms of structural relaxation are discussed.

1. INTRODUCTION

Figure 1 shows schematically the temperature dependence of the shear viscosity, η , in a typical amorphous metallic system. As the liquid is cooled below its melting point, T_m , its viscosity rises rapidly. Although the liquid below T_m is metastable with respect to the crystalline state, it is still in internal equilibrium, the atomic configuration changing with temperature, until η reaches $\sim 10^{11} \text{ Nsm}^{-2}$ when the necessary configurational rearrangements become so slow. Below this *glass transition temperature*, T_g , η continues to rise, but more slowly, because the glass is in an *isoconfigurational* state. A faster quenched liquid will go through the glass transition sooner, e.g., following line 1; a more slowly quenched glass might follow line 2. The glass in state 1 or 2 can be assigned a *fictive temperature*, T_f , defined as the intersection of the isoconfigurational and equilibrium lines.

Metallic glasses (amorphous alloys), whether produced by rapid quenching of

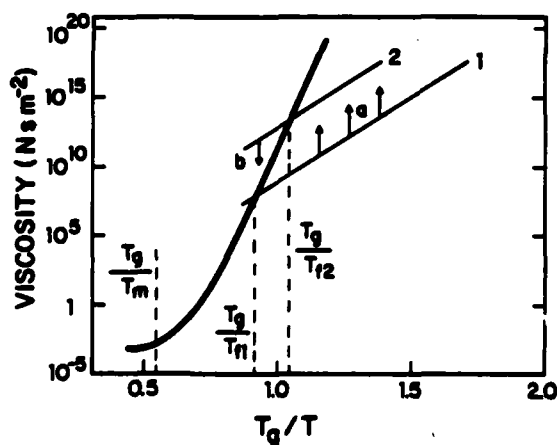


FIGURE 1
Schematic temperature dependence of the shear viscosity in an amorphous metallic system.

the melt or by sputtering or vapor deposition, are configurationally frozen far from internal equilibrium. Given sufficient atomic mobility (on annealing) they can lower their free energy by altering their amorphous structure. This *structural relaxation* is manifested by significant changes in many properties. To understand the mechanisms of structural relaxation, studies of atomic transport (i.e., viscous flow and diffusion) are essential. A major hindrance to the

TABLE 1
Effects of Structural Relaxation

Property	Relaxation Behavior*						Selected References
	A**	B	C	D	E	F	
Density	I						3
Enthalpy	D		✓	✓		✓	4,5,6
Young's modulus	I		✓	✓	✓		7,8,9
Diffusivity	D						10,11
Viscosity	I	✓					12,13,14
Curie temperature	I,D	✓	✓	✓	✓	✓	15,16,17,18
Electrical resistivity	I,D		✓	✓			19,20,21
Rate of stress relief	D					✓	22,23
Internal friction	D						24
Ductility	D		✓	✓			25,26
Magnetic after-effect	D		✓			✓	27,28
Induced magnetic anisotropy			✓	✓			29
X-ray structure factor	✓						30,31
Superconducting transition temperature	D		✓				32

*The column headings are explained in Section 2.1.

**I,D indicate an increase or decrease.

measurement of relaxation and of atomic transport is the tendency of metallic glasses to crystallize.

In this paper, data on relaxation effects, viscous flow and diffusion are reviewed and analyzed. Attention is restricted to glasses of the metal-metalloid type, i.e., those containing ~80 at.% of one or a mixture of noble or late transition metals (e.g., Au, Co, Fe, Mn, Ni, Pd, Pt, Ru) and ~20 at.% of one or a mixture of metalloids (e.g., B, C, Ge, P, Si). These glasses have been the most widely studied.^{1,2}

2. STRUCTURAL RELAXATION

2.1. Survey of Phenomena

On annealing metallic glasses, many property changes have been observed and have been attributed to structural relaxation (see Table 1). The main types of behavior are described below.

A. Irreversible relaxation. Many properties undergo "irreversible" changes on annealing, the changes being larger and faster at higher annealing temperatures. At each temperature the property change is initially rapid and slows down progressively, though there is no marked tendency for the property to stabilize at a final value. This type of relaxation occurs on annealing below T_g and is indicated by the arrows (a) in Fig. 1. The glass is relaxing toward equilibrium, but is far from achieving it. "Monotonic" relaxation would be a better description than "irreversible", because suitable annealing treatments may partially reverse the property changes as in (B).

B. Reversible relaxation near T_g . A relatively relaxed (low fictive temperature) glass, e.g., on isoconfigurational line 2 in Fig. 1, may be heated rapidly along the line so that reverse relaxation (arrow b) toward equilibrium may occur. For any property, in principle, reversible changes between states on the equilibrium line may be obtained in the vicinity of T_g . Because of rapid crystallization in this temperature range, reversibility has been observed only rarely.

C. Reversible relaxation below T_g . In some cases reversible property changes have been observed at temperatures up to 150K below T_g . Because crystallization is less of a problem, it has been possible to cycle repeatedly between two temperatures and corresponding "equilibrium" property values. This low temperature relaxation seems distinct from that occurring nearer T_g .

D. Relaxation of kinetics. Although the relaxations near T_g and below T_g may be distinct, they are not independent. The kinetics of type (C) relaxation are slower in samples which are more relaxed according to type (A). This is in accord with the observation that type (A) relaxation reduces atomic mobility.

E. Memory effect. In an experiment to demonstrate the "memory" or "crossover" effect, a metallic glass is annealed until the property being measured attains a value characteristic of "equilibrium" at a higher annealing temperature. In subsequent annealing at the higher temperature, it is found that the initial property change first reverses somewhat before the equilibrium value is reestablished. This shows that one parameter, the value of a property or the fictive temperature, is not sufficient to specify the structural state of the glass. That more than one parameter (in addition to temperature and pressure) is required is a characteristic also of other, more conventional glasses.³³

F. Quench rate effects. The properties of a metallic glass depend on the mode of production, in particular on the effective quench rate. As expected from Fig. 1, the property differences on going from fast-quenched to slow-quenched glasses are, in general, analogous to the changes brought about by annealing.

2.2. Analysis

It is expected that reversible property changes could be observed near T_g . In metallic glasses, however, reversible changes have been observed at lower temperature, and different properties may show irreversible and reversible changes at the same temperature. It could be considered that the materials have a distribution of T_g 's.³⁴ The kinetics of property changes can be analyzed into a spectrum of relaxation times. For resistivity changes in $\text{Fe}_{40}\text{Ni}_{40}\text{P}_{14}\text{B}_6$ glass four peaks in the spectrum have been found,³⁵ but the general problem of relating the relaxation times to atomic mechanisms remains. In

considering a range of relaxation processes with a wide spread in their kinetics (as in metallic glasses) a distribution of activation energies is a more useful description than a fixed activation energy with a distribution of pre-factors.³⁶ Gibbs et al.³⁷ have taken this approach and developed a model for property changes, based on changes in the number density of processes distributed in activation energy. To a good approximation, it is shown that on annealing at a temperature T for time t , only processes with activation energy less than $kT \ln(\nu t)$ can occur, where ν is an atomic vibration frequency. The changes brought about by annealing have reversible and irreversible components and the model is capable of explaining, in a general way, all of the observed relaxation phenomena with the exception of type (D). This exception, which is the main drawback of the model, arises from the assumption that the processes are independent. This is unlikely for configurational rearrangements in a real structure.

The approach of Gibbs et al. does not give any information on mechanisms. As described above, there may be two distinct types of relaxation. Egami³⁸ proposed a distinction between: *topological short range ordering* (TSRO), a rearrangement of the topology of the glassy structure; and *compositional short range ordering* (CSRO), a rearrangement of different chemical species not affecting the topology. CSRO involving only nearest neighbor atoms would be more rapid and could explain type (C) relaxation. Types (A) and (B) would be attributed to TSRO. The terms TSRO and CSRO will be retained in this paper, though others have been proposed.^{5,15,16} Most attention has been devoted to TSRO. The theoretical models are based on defects,³⁹ which are deviations from the ideal glassy structure. Atomic transport is attributed to the motion of defects and structural relaxation (type (A)) to their annihilation. In order to allow type (B) relaxation, and to avoid atomic mobilities of zero, it is necessary that the thermal equilibrium population of defects be non-zero. The most widely used description of atomic transport and structural relaxation is based on the free volume theory for simple liquids⁴⁰ (discussed in Section 3.1). An alternative approach is based on the description of the local structure in terms of atomic level stresses:¹⁵ positive and negative density fluctuations and shear defects have been identified, but their relationships to atomic transport and relaxation *kinetics* have not been established. The mechanisms of CSRO and TSRO will be discussed further in Section 4, after a consideration of direct measurements of atomic transport.

3. ATOMIC TRANSPORT

3.1. Viscous Flow

The viscosity of metallic glasses can increase by 5 orders of magnitude on annealing;⁴¹ this is certainly the most dramatic property change due to structural relaxation. Using a creep test, Taub and Spaepen¹² measured the homogeneous viscous flow of $\text{Pd}_{82}\text{Si}_{18}$ glass at selected temperatures in the range 424-537K, well below $T_g = 642\text{K}$. At each temperature the viscosity, η , rose linearly with time. When the fractional rise in viscosity, $d \ln \eta / dt$, became sufficiently low, it was possible to change the temperature of the test, measure η at the new temperature, and then return to the original temperature to find that η had not changed measurably. By making several excursions in this manner it was possible to obtain the isoconfigurational variation of η with temperature. It may seem surprising that relaxation is negligible while it is possible to measure viscous flow, but only $\sim 10^{-4}$ jumps/atom are required for a viscosity measurement. Taub and Spaepen¹² found that the temperature dependence of the isoconfigurational viscosity was Arrhenian, with an activation energy, 192 kJmol^{-1} , independent of the degree of relaxation. Similar measurements have been made on other systems.⁴²

The rise of viscosity on annealing ((a) in Fig. 1) is most easily attributed to the annealing out of "flow defects".³⁹ These defects are sites at which shear can occur (Fig. 2), and could arise when the local free volume exceeds a critical value.¹² By fitting the stress-strain rate behavior it is found that $\gamma_0 \Omega_F$ ($\gamma_0 \dots$ local shear strain; $\Omega_F \dots$ volume of defect) is 2-8 atomic volumes.⁴² These values of $\gamma_0 \Omega_F$ are reasonable for extensive shear in a small volume (as in Fig. 2), but are also consistent with a small shear in a larger volume. The annihilation of flow defects may occur at "relaxation defects". The linear rise of η indicates bimolecular kinetics in which the population, n_f , of flow defects obeys $\dot{n}_f = n_f^2$. It is necessary to assume that the population of relaxation defects is proportional to n_f .

Tsao and Spaepen^{13,14} extended the measurements of Taub and Spaepen to higher temperatures, closer to T_g . The onset of crystallization was a problem, though less serious in $\text{Pd}_{77.5}\text{Cu}_6\text{Si}_{16.5}$ than in $\text{Pd}_{82}\text{Si}_{18}$. It was found that the isoconfigurational temperature dependence of η was markedly non-Arrhenian, demonstrating that n_f is not constant. In addition, the isothermal increases in viscosity began to saturate. The kinetics of the increase were still best described as bimolecular, but it was necessary to assume that n_f was decaying not to zero, but to a finite equilibrium value.¹⁴ Onset of crystallization prevented the attainment of equilibrium, but it was possible to estimate the equilibrium viscosity, η_{eq} , by extrapolation (Fig. 3). In highly relaxed samples, it was possible to observe reverse relaxation corresponding to (b) in

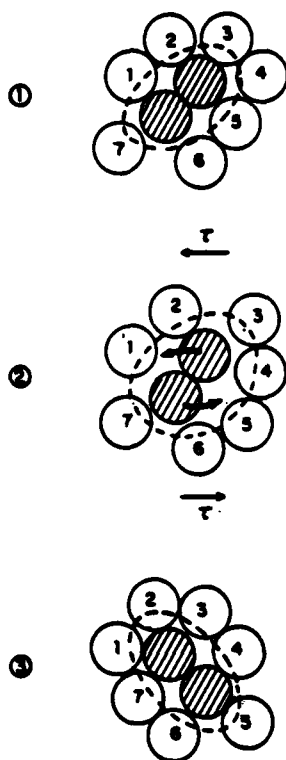


FIGURE 2
Schematic diagram showing
the motion of a flow defect
under the action of a shear
stress. After Spaepen.³⁹

Fig. 1 (Fig. 3).⁴³ The kinetics of this relaxation could be adequately described as bimolecular or unimolecular, but, most significantly, the curve extrapolated to the same equilibrium value as the approach from lower viscosity.⁴³ Thus, despite the problems with crystallization (Fig. 3), reversible relaxation of η near T_g has been demonstrated. The temperature variation of extrapolated η_{eq} 's obeys the Fulcher-Vogel expression, as expected from the free volume theory.

Bimolecular (increasing η) and unimolecular (decreasing η) kinetics have been observed in relaxation of amorphous covalently bound systems,¹⁴ and are easily interpreted if broken bonds constitute the flow defects. Given strong metal-metalloid bonding, flow defects in metallic glasses might also be considered as broken bonds in a continuous random network.¹⁴

3.2. Diffusion

A large number of diffusion coefficients have now been measured in metallic glasses (for a recent review see ⁴⁴). Annealing temperatures must be below T_g to avoid crystallization, and consequently the diffusion coefficients are typically less than $10^{-20} \text{m}^2 \text{s}^{-1}$. To detect such low diffusivities by conventional means requires special techniques for the measurement of composition profiles of small spatial extent.⁴⁴ The resolution limit of most analysis techniques is $\sim 30 \text{\AA}$, and with penetration distances of that order, it is possible to measure diffusivities as low as $10^{-24} \text{m}^2 \text{s}^{-1}$.

The use of artificial compositionally modulated materials provides an even more sensitive measure of diffusion. Such materials have been made, for example, by sputter deposition of alternate layers of $\text{Pd}_{85}\text{Si}_{15}$ and $\text{Fe}_{85}\text{B}_{15}$ glasses.¹¹ The decay of the composition modulation is measured by monitoring the decay of the X-ray satellite due to the modulation, and effective interdiffusivities, \bar{D}_λ , down to $10^{-27} \text{m}^2 \text{s}^{-1}$ can be measured. The values of \bar{D}_λ depend on the modulation wavelength, λ , and the form of the dependence gives useful thermodynamic information.⁴⁵ Extrapolation of \bar{D}_λ to $\lambda = \infty$ gives \bar{D} , the bulk interdiffusivity, and values of \bar{D} are in good agreement with diffusivities measured in comparable conventional experiments.⁴⁵

On the basis of the viscosity results (Section 3.1), it is expected that

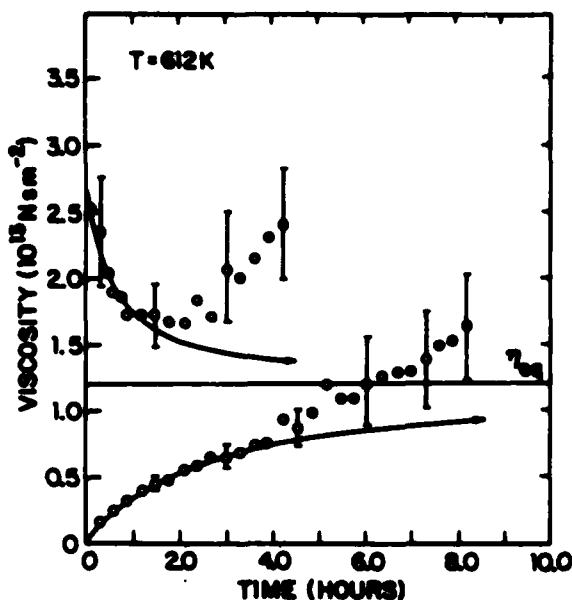


FIGURE 3
Relaxation of the viscosity of
 $\text{Pd}_{77.5}\text{Cu}_6\text{Si}_{16.5}$ glass at 612K. The
curves indicate bimolecular
kinetics. Deviations from the
curves are due to crystallization.
After Teo and Spaspen.⁴³

diffusivities should decrease on structural relaxation. Early Rutherford backscattering measurements of the diffusivity of Au in $\text{Pd}_{77.5}\text{Cu}_6\text{Si}_{16.5}$ showed a fifty-fold decrease as a result of pre-annealing.¹⁰ This result has not been confirmed by later work, nor have significant relaxation effects been found in conventional measurements of diffusivities in other systems.⁴⁴ With compositionally modulated glasses, however, the interdiffusivity \bar{D} can be monitored continuously, and decreases in \bar{D} by a factor of ~ 150 have been observed during annealing.¹¹ A linear rise of $1/\bar{D}$ with time was found. The time required to obtain a diffusivity measurement by a composition profiling technique is such that the average number of jumps/atom in the

specimen is at least 200. By contrast, only 0.2 jumps/atom are necessary for an interdiffusivity measurement using a modulated material. Thus it is notable, but not surprising, that relaxation effects can be observed with the latter technique, but not with the former because of substantial relaxation during the diffusion anneal.

Isoconfigurational measurements of diffusivity are possible only using the modulated film technique. Cycling the temperature as for the viscosity measurements, the isoconfigurational temperature dependence of \bar{D} was determined in a $\text{Pd}_{85}\text{Si}_{15}/\text{Fe}_{85}\text{B}_{15}$ film.¹¹ The behavior was Arrhenian, with an activation energy, 195 kJmol^{-1} , very close to that for viscous flow in $\text{Pd}_{82}\text{Si}_{18}$.¹²

The majority of diffusion measurements have been made using composition profiling techniques, and by the nature of this method, were made on relaxed samples. It has been suggested that the diffusivities fall into two groups: fast diffusion of small atoms (generally metalloid) by an interstitial mechanism; and slow diffusion of large atoms (generally metal) by a substitutional mechanism.⁴⁶ Later data do not support this distinction. Figure 4 shows that the metal and metalloid diffusivities in Fe-based glasses are remarkably close, compared to substitutional and interstitial rates in crystalline iron.⁴⁷ It appears that the metalloid atoms in metal-metalloid glasses do not diffuse

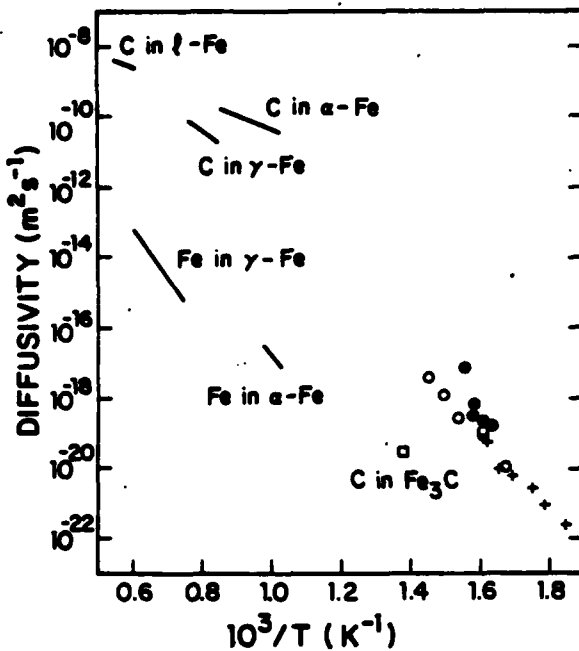


FIGURE 4
 Comparison of diffusivities in Fe-based systems: Fe in $Fe_{40}Ni_{40}P_{14}B_6$ (+);⁵⁵
 B in $Fe_{40}Ni_{40}B_{20}$ (•);⁵⁶
 Si in $Fe_{82}B_{12}Si_6$ (○);⁵⁷
 other data from refs. 47, 49, 58.

interstitially, but that their movement is linked to that of the metal atoms. This is not surprising in view of the strong metal-metalloid bonding in these systems and the high degree of chemical short range order.⁴⁸ No metalloid-metalloid nearest neighbor pairs are found; it has been suggested that each metalloid atom is surrounded by a trigonal prism of metal atoms, as in the crystalline compounds of similar composition. Unfortunately, there is a lack of data on metalloid diffusion in crystalline metal-metalloid compounds, though one diffusivity, that of C in Fe_3C , has been reported recently, and indeed it is remarkably low.⁴⁹ The description of interstitial diffusional jumps in a dense random packed structure has been

attempted,⁵⁰ and it is likely that the results will be useful in interpreting data on the diffusion of H and other small foreign atoms. For metalloids which are a component of the structure, however, it appears that an interstitial mechanism is not operative. As in interpreting viscosity measurements, it may be appropriate to think of the glass structure as a connected network; at defects in the network (analogous to broken bonds in silicates) diffusional jumps of both metal and metalloid atoms are possible.

3.3. Relationship Between Diffusion and Viscous Flow

The relationship between the rates of atomic diffusion and of viscous flow is very important for understanding atomic transport mechanisms. In the free volume theory, which has been used so successfully in interpreting viscosity measurements,¹² diffusion and viscous flow occur by the same mechanism (e.g., Fig. 2) and it is expected that the Stokes-Einstein relationship will apply:

$$\eta D = \frac{kT}{6\pi r}, \quad (1)$$

where r is a characteristic particle radius. Equation (1) works quite well ($\pm 50\%$) for several liquid metals⁵¹ if an average ionic radius is chosen for r . Chen et al.¹⁰ measured the diffusivity of Au in $Pd_{77.5}Cu_6Si_{16.5}$ just above T_g and compared it with the viscosity of the glass in the same temperature range.

They found $r = 0.42\text{\AA}$, in reasonable agreement with the expected value of 0.72\AA (average of Pd^{2+} and Pd^{4+} radii). A comparison of more recent viscosity¹⁴ and diffusion data,⁴⁴ however, suggests that $r \approx 10^{-4}\text{\AA}$. It is difficult to interpret these results because the degree of relaxation in the samples was not standardized. Since η in $\text{Pd}_{82}\text{Si}_{18}$ glass¹² and $1/\bar{D}$ in a $\text{Pd}_{85}\text{Si}_{15}/\text{Fe}_{85}\text{B}_{15}$ modulated film^{11,52} both rise linearly with annealing time, it is possible to compare the rates of increase without concern about the degree of relaxation. Data on the decay of satellite intensities in modulated film samples¹¹ were fitted assuming Eq. 1 to be valid and using two adjustable parameters: the radius, r , in Eq. 1; and the initial viscosity. Good fits were obtained with $r = 4.4 \times 10^{-13}\text{m}$ at 573K, and $r = 1.2 \times 10^{-13}\text{m}$ at 523K; i.e., the measured diffusivity was $\sim 160\times$ and $\sim 590\times$ the values which would be predicted using an ionic radius in Eq. 1.

Although more data are required, particularly diffusivities and viscosities in the same glass with the same degree of relaxation, it seems likely that the Stokes-Einstein relationship is not valid for metal-metalloid glasses, at least well below T_g . Measured diffusivities are significantly greater than would be expected from measured viscosities, i.e., there are diffusive jumps which do not contribute to flow. One speculation on the diffusion mechanism is that it could involve the movement of vacant sites on the metal-metalloid network, which could occur without substantial alteration of the topology of the network. Computer models have shown that a vacancy is not stable in a monatomic glass,⁵³ but it is not known whether this is true in a glass with strong chemical short range order. It is worth noting that the pre-exponential diffusivity determined in modulated film studies⁴⁵ is $5.6 \times 10^{-5}\text{m}^2\text{s}^{-1}$, a reasonable value for a singly activated process.

In a crystal, viscous flow can occur through the movement of vacancies. This is Nabarro-Herring creep, in which the viscosity is given by⁵⁴

$$\eta = \frac{kTd^2}{4\Omega D}, \quad (2)$$

where Ω is the atomic volume and d is the grain size. The grain boundaries act as sources and sinks for vacancies. Comparing η and D for a metallic glass, using relaxation rates, as above, it is found that the characteristic distance, d , is $\sim 30\text{\AA}$ at 573K and $\sim 50\text{\AA}$ at 523K. In metal-metalloid glasses there could be a link between D and η analogous to that in Nabarro-Herring creep, but it seems likely that, in addition, atom movement of the type shown in Fig. 2 occurs and contributes to both diffusion and viscous flow.

To determine physically meaningful activation energies, it is necessary to use *isocofigurational* measurements. When these have been made the activation energies for viscous flow and for diffusion have been found to be the same.¹¹

Since both η and $1/D$ rise linearly on relaxation below T_g , it appears that the rates of viscous flow and diffusion scale. A full understanding of diffusion and viscous flow should include these effects.

4. DISCUSSION

It is now possible to come to some conclusions on the nature of the two types of relaxations referred to in Section 2.2.

The glass transition is closely related to viscosity (Fig. 1), and it appears that the relaxation, reversible and irreversible, near T_g is best attributed to changes in the population of flow defects, i.e., the defects responsible for viscous flow. This relaxation does affect the structure of metal-metalloid glasses in a measurable way;³⁰ its description as *topological* (i.e. TSRO) would appear to be well founded. The free volume theory has been applied very successfully to describe the viscosity relaxation. Below T_g isothermal annealing causes a linear increase in viscosity, and the free volume decreases calculated from this are consistent with observed increases in density,¹² increases in Curie temperature,¹⁶ and changes in electrical resistivity.²⁰ Van den Beukel and Radelaar⁶ have extended the free volume model to non-isothermal relaxation, and have considered how the free volume might affect the kinetics of the other relaxation process, CSRO. Their model has been applied successfully to calorimetric data.

The reversible relaxation below T_g has been attributed to the short range ordering of chemical species on the random network, analogous to clustering or ordering on a crystalline lattice. This CSRO is too rapid to be governed by the same mechanism as TSRO. It has been suggested that it could occur by minor cooperative atomic rearrangement.¹⁵ An alternative is that the ordering could occur by diffusive jumps, governed by the movement of defects analogous to vacancies in crystals. As pointed out above, there are diffusive jumps which do not contribute to viscous flow. Direct structural evidence for CSRO is difficult to obtain,¹⁵ but some recent work with compositionally modulated films may offer some insight. From the dependence of \bar{D}_λ on λ for $\text{Pd}_{85}\text{Si}_{15}/\text{Fe}_{85}\text{B}_{15}$ films it has been shown that this is an *ordering* system^{45,52} (i.e., with a negative enthalpy of mixing). In a small wavelength ($\lambda = 2.275\text{\AA}$) film, the decay of the artificial composition modulation at longer times has been attributed to ordering within the layers.⁵² The relaxation time for this decay is $\sim 300\text{s}$ at 523K. The interdiffusion coefficient at this temperature is $1.94 \times 10^{-24}\text{m}^2\text{s}^{-1}$, giving a mean time between consecutive atomic jumps of $\sim 600\text{s}$. Thus the diffusion coefficient appears to be consistent with the kinetics of CSRO.

Although in the modulated film the ordering was detected through its influence on the metal atoms, it is likely that the metal-metalloid bonding is very

important. From calorimetric studies there is evidence that CSRO does not occur in a glass with only one metal and one metalloid, does occur when a third species (metal or metalloid) is added, and is stronger the more components there are.⁴ It appears from the viscosity relaxation kinetics, and from the relationship between viscous flow and diffusion, that metal-metalloid glasses do not behave as simple liquids and that the role of the metal-metalloid bonding must be considered.

ACKNOWLEDGEMENTS

It is a pleasure to thank S. Radelaar, F. Spaepen and D. Turnbull for useful discussions. I am grateful to S.S. Tsao and F. Spaepen for permission to quote their results prior to publication. The author's research in this area has been supported by the Office of Naval Research under Contract N00014-77-C-0002.

REFERENCES

- 1) Proc. 4th Int. Conf. on Rapidly Quenched Metals (Sendai, 1981) eds. T. Masumoto and K. Suzuki (Japan Inst. of Metals, 1982).
- 2) F.E. Luborsky (ed.) Amorphous Metallic Alloys (Butterworths, London, 1983).
- 3) H.S. Chen, J. Appl. Phys. 49 (1978) 3289.
- 4) I. Majewska, B.J. Thijsse and S. Radelaar, in: Ref. [1] pp. 483-486.
- 5) H.S. Chen, in: Ref. [2] pp. 169-186.
- 6) A. van den Beukel and S. Radelaar, Acta Metall. 31 (1983) 419.
- 7) A. Kursumovic, M.G. Scott, E. Girt and R.W. Cahn, Scripta Metall. 14 (1980) 1303.
- 8) M.G. Scott, R.W. Cahn, A. Kursumovic, E. Girt and N.B. Njuhovic, in: Ref. [1], pp. 469-474.
- 9) A.L. Mulder, S. van der Zwaag and A. van den Beukel, this volume.
- 10) H.S. Chen, L.C. Kimerling, J.M. Poate and W.L. Brown, Appl. Phys. Lett. 32 (1978) 461.
- 11) A.L. Greer, C.-J. Lin and F. Spaepen, in: Ref. [1] pp. 567-572.
- 12) A.I. Taub and F. Spaepen, Acta Metall. 28 (1980) 1781.
- 13) S.S. Tsao and F. Spaepen, in: Ref. [1] pp. 463-468.
- 14) S.S. Tsao and F. Spaepen, in: Modeling the Structure and Properties of Amorphous Materials, ed. V. Vitek (Trans. A.I.M.E. Symp. Proc., 1983) in press.
- 15) T. Egami, in: Ref. [2] pp. 100-113.
- 16) A.L. Greer and F. Spaepen, Ann. N.Y. Acad. Sci. 371 (1981) 218.
- 17) Y.-N. Chen and T. Egami, J. Appl. Phys. 50 (1979) 7615.
- 18) A.L. Greer, J. Mater. Sci. 17 (1982) 1117.
- 19) M. Balanzat, Scripta Metall. 14 (1980) 173.
- 20) K.F. Kelton and F. Spaepen, in: Ref. [1] pp. 527-530.
- 21) M.E. Sonius, B.J. Thijsse, A. van den Beukel, Scripta Metall. 17 (1983) 545.
- 22) R.S. Williams and T. Egami, IEEE Trans. Magn. MAG-12 (1976) 927.
- 23) F.E. Luborsky and J.L. Walter, Mater. Sci. Eng. 35 (1978) 255.
- 24) B.S. Berry and W.C. Pritchett, J. Appl. Phys. 44 (1973) 3122.
- 25) F.E. Luborsky and J.L. Walter, J. Appl. Phys. 47 (1976) 3648.
- 26) A.L. Mulder, S. van der Zwaag and A. van den Beukel, to be published.
- 27) P. Allia, F.E. Luborsky, R. Sato Turtellif, G.P. Soardo and F. Vinai, IEEE Trans. Magn. MAG-17 (1981) 2615.
- 28) N. Moser and H. Kronmüller, J. Magn. Magn. Mat. 19 (1980) 275.

- 29) W. Chambron and A. Chamberod, *J. Phys.* 41(C8) (1980) 710.
- 30) T. Egami, *J. Mater. Sci.* 13 (1978) 2587.
- 31) E. Chason, Harvard University, Personal Communication.
- 32) S.J. Poon, in: Ref. [2] pp. 432-450.
- 33) A.L. Greer and J.A. Leake, *J. Non-Cryst. Sol.* 33 (1979) 291.
- 34) H.S. Chen, in: Ref. [1] pp. 495-500.
- 35) J.R. Cost and J.T. Stanley, in: Ref. [1] pp. 491-494; this volume.
- 36) A.S. Argon and H.Y. Kuo, *J. Non-Cryst. Sol.* 37 (1980) 241.
- 37) M.R.J. Gibbs, J.E. Evetts and J.A. Leake, *J. Mater. Sci.* 18 (1983) 278; this volume.
- 38) T. Egami, *Mater. Res. Bull.* 13 (1978) 557.
- 39) F. Spaepen, in: *Physics of Defects*, ed. R. Balian et al., Les Houches Lectures XXXV (North-Holland, Amsterdam, 1981) pp. 133-174.
- 40) D. Turnbull and M.H. Cohen, *J. Chem. Phys.* 52 (1970) 3038.
- 41) A.I. Taub and F. Spaepen, *Scripta Metall.* 13 (1979) 195.
- 42) F. Spaepen and A.I. Taub, in: Ref. [2] pp. 231-256.
- 43) S.S. Tsao and F. Spaepen, Personal Communication.
- 44) B. Cantor and R.W. Cahn, in: Ref. [2] pp. 487-505.
- 45) R.C. Cammarata and A.L. Greer, this volume.
- 46) M. Kijek, M. Ahmadzadeh, B. Cantor and R.W. Cahn, *Scripta Metall.* 14 (1980) 1337.
- 47) R.W.K. Honeycombe, *Steels* (Edward Arnold, London, 1981).
- 48) P.H. Gaskell, *J. Non-Cryst. Sol.* 32 (1979) 207.
- 49) B. Ozturk, V.L. Fearing, J.A. Ruth and G. Simkovich, *Met. Trans. A* 13A (1982) 1871.
- 50) M. Ahmadzadeh and B. Cantor, in: Ref. [1] pp. 591-594.
- 51) N.H. Nachtrieb, in: *Liquid Metals and Solidification* (ASM, Cleveland, 1958) p. 49.
- 52) A.L. Greer, in: *Modulated Structure Materials*, ed. T. Tsakalakos, NATO ASI Series, Applied Sciences (Martinus Nijhoff, The Hague, 1983) in press.
- 53) C.H. Bennett, P. Chaudhari, V. Moruzzi and P. Steinhardt, *Phil. Mag. A* 40 (1979) 485.
- 54) A.H. Cottrell, *The Mechanical Properties of Matter* (Wiley, New York, 1964).
- 55) P. Valenta, K. Maier, H. Kronmüller and K. Freitag, *Phys. Stat. Sol.* 106 (1981) 129.
- 56) R.W. Cahn, J.E. Evetts, J. Patterson, R.E. Somekh, C. Kerway Jackson, *J. Mater. Sci.* 15 (1980) 702.
- 57) F.E. Luborsky and F. Bacon, in: Ref. [1] pp. 561-566.
- 58) G.S. Ershov and A.A. Kasatkin, *Stal.* 8 (1977) 712.

Defense Documentation Center
Cameron Station
Alexandria, Virginia 22304 (12)

Office of Naval Research
Department of the Navy
Attn: Code 471 (23)
Code 470 (45)

Director
Office of Naval Research
Branch Office
495 Summer Street
Boston, Massachusetts 02210

Director
Office of Naval Research
Branch Office
134 South Clark Street
Chicago, Illinois 60605

Office of Naval Research
San Francisco Area Office
165 Market Street, Room 447
San Francisco, California 94102

Naval Research Laboratory
Washington, D. C. 20390
Attn: Code 6000
Code 6100
Code 6300
Code 6400
Code 2537 (45)

Attn: Mr. F. S. Williams
Naval Air Development Center
Code 302
Warminster, Pennsylvania 18974

Naval Air Propulsion Test Center
Trenton, New Jersey 08625
Attn: Library

Naval Weapons Laboratory
 Dahlgren, Virginia 22445
Attn: Research Division

Naval Construction Battalion
Civil Engineering Laboratory
Port Hueneme, California 93043
Attn: Materials Division

Naval Electronics Laboratory Center
San Diego, California 92152
Attn: Electronic Materials Sciences Div.

Naval Missile Center
Materials Consultant
Code 3312-1
Point Mugu, California 93041

Commanding Officer
Naval Ordnance Laboratory
White Oak
Silver Spring, Maryland 20910
Attn: Library

Naval Ship B. and D. Center
Materials Department
Annapolis, Maryland 21402

Naval Undersea Center
San Diego, California 92132
Attn: Library

Naval Underwater System Center
Navpact, Rhode Island 02840
Attn: Library

Naval Weapons Center
China Lake, California 93555
Attn: Library

Naval Postgraduate School
Monterey, California 93940
Attn: Materials Sciences Dept.

Naval Air Systems Command
Washington, D. C. 20360
Attn: Code 52031
Code 52032
Code 330

Naval Sea System Command
Washington, D. C. 20362
Attn: Code 030

Naval Facilities
Engineering Command
Alexandria, Virginia 22331
Attn: Code 03

Scientific Advisor
Commandant of the Marine Corps
Washington, D. C. 20380
Attn: Code AX

Naval Ship Engineering Center
Department of the Navy
Washington, D. C. 20360
Attn: Director, Materials Sciences

Army Research Office
Box CM, Dade Station
Durham, North Carolina 27706
Attn: Metallurgy and Ceramics Div.

Army Materials and Mechanics
Research Center
Watertown, Massachusetts 02172
Attn: Res. Programs Office (AMMRR-P)

Commanding General
Demcorad of the Army
Frickford Arsenal
Philadelphia, Pennsylvania 19137
Attn: OADBA-1320

Office of Scientific Research
Department of the Air Force
Washington, D. C. 20333
Attn: Solid State Div. (SRSP)

Aerospac Research Labs
Wright-Patterson AFB
Building 450
Dayton, Ohio 45433

Air Force Materials Lab (LA)
Wright-Patterson AFB
Dayton, Ohio 45433

MSA Headquarters
Washington, D. C. 20546
Attn: Code RRM

MSA
Lewis Research Center
11200 Brimley Road
Cleveland, Ohio 44135
Attn: Library

National Bureau of Standards
Washington, D. C. 20234
Attn: Metallurgy Division
Inorganic Materials Division

Atomic Energy Commission
Washington, D. C. 20545
Attn: Metals and Materials Branch

Defense Metals and Ceramics
Information Center
Battelle Memorial Institute
505 King Avenue
Columbus, Ohio 43201

Director
Ordnance Research Laboratory
P. O. Box 30
State College, Pennsylvania 16801

Director Applied Physics Lab.
University of Washington
1013 Northeast Forteth Street
Seattle, Washington 98105

Metals and Ceramics Division
Oak Ridge National Laboratory
P. O. Box X
Oak Ridge, Tennessee 37830

Los Alamos Scientific Lab.
P. O. Box 1663
Los Alamos, New Mexico 87546
Attn: Report Libraries

Argonne National Laboratory
Metallurgy Division
P. O. Box 225
Lemont, Illinois 60439

Brockhaven National Laboratory
Technical Information Division
Upton, Long Island
New York 11973
Attn: Research Library

Library
Building 30, Room 134
Lawrence Radiation Laboratory
Berkeley, California

Professor G. S. Ansell
Rensselaer Polytechnic Institute
Dept. of Metallurgical Engineering
Troy, New York 12181

Professor H. K. Birnbaum
University of Illinois
Department of Metallurgy
Urbana, Illinois 61801

Dr. E. M. Breiman
United Aircraft Corporation
United Aircraft Research Lab.
East Hartford, Connecticut 06108

Professor H. D. Brody
University of Pittsburgh
School of Engineering
Pittsburgh, Pennsylvania 15213

Professor J. B. Cohen
Northwestern University
Dept. of Material Sciences
Evanston, Illinois 60201

Professor M. Cohen
Massachusetts Institute of Technology
Department of Metallurgy
Cambridge, Massachusetts 02139

Professor B. C. Gleason
Northwestern University
Department of Chemistry
Boston, Massachusetts 02115

Dr. O. T. Hahn
Battelle Memorial Institute
Department of Metallurgy
515 King Avenue
Columbus, Ohio 43201

Professor R. W. Nechal
Carnegie-Mellon University
Scholarly Park
Pittsburgh, Pennsylvania 15213

Dr. David G. Hovden
Battelle Memorial Institute
Columbus Laboratories
505 King Avenue
Columbus, Ohio 43201

Professor C. E. Jackson
Ohio State University
Dept. of Welding Engineering
190 West 19th Avenue
Columbus, Ohio 43210

Professor G. Judd
Rensselaer Polytechnic Institute
Dept. of Materials Engineering
Troy, New York 12181

Dr. C. S. Korvath
TRW, Inc.
23555 Euclid Avenue
Cleveland, Ohio 44117

Professor D. A. Koss
Michigan Technological University
College of Engineering
Houghton, Michigan 49931

Professor A. Lawley
Drexel University
Dept. of Metallurgical Engineering
Philadelphia, Pennsylvania 19104

Dr. H. Margalla
Polytechnic Institute of New York
333 Jay Street
Brooklyn, New York 11201

Professor K. Masabuchi
Massachusetts Institute of Technology
Department of Ocean Engineering
Cambridge, Massachusetts 02139

Dr. G. H. Meyer
University of Pittsburgh
Dept. of Metallurgical and Materials
Engineering
Pittsburgh, Pennsylvania 15213

Professor J. W. Morris, Jr.
University of California
College of Engineering
Berkeley, California 94720

Professor K. Ono
University of California
Materials Department
Los Angeles, California 90024

Professor W. F. Savage
Rensselaer Polytechnic Institute
School of Engineering
Troy, New York 12181

Dr. C. Shaw
Reichart International Corp.
P. O. Box 1083
1045 Camino Del Rio
Thousand Oaks, California 91340

Professor O. D. Sherby
Stanford University
Materials Science Dept.
Stanford, California 94305

Professor J. Shyne
Stanford University
Materials Science Department
Stanford, California 94305

Dr. W. A. Spitzig
U.S. Steel Corporation
Research Laboratory
Monroeville, Pennsylvania 15146

Dr. E. A. Starke, Jr.
Georgia Institute of Technology
School of Chemical Engineering
Atlanta, Georgia 30332

Professor H. S. Stone
Rensselaer Polytechnic Institute
School of Engineering
Troy, New York 12181

Dr. E. R. Thompson
United Aircraft Research Lab.
400 Main Street
East Hartford, Connecticut 06108

Professor David Turnbull
Harvard University
Division of Engineering and Applied
Physics
Cambridge, Massachusetts 02139

Dr. F. W. Wang
Naval Ordnance Laboratory
Physics Laboratory
White Oak
Silver Spring, Maryland 20910

Dr. J. C. Williams
Reichart International
Science Center
P. O. Box 1083
Thousand Oaks, California 91340

Professor M. C. F. Windsor
University of Virginia
Department of Materials Science
Charlottesville, Virginia 22903

Dr. M. A. Wright
University of Tennessee
Space Institute
Dept. of Metallurgical Engineering
Tullahoma, Tennessee 37388

END

FILMED

2-84

DTIC